

New Models for Wolf-Rayet and O Star Populations in Young Starbursts

Daniel Schaerer

Space Telescope Science Institute, 3700 San Martin Drive, Baltimore, MD 21218, USA

and

William D. Vacca³

Institute for Astronomy, Honolulu, HI 96822, USA

ABSTRACT

Using the latest stellar evolution models, theoretical stellar spectra, and a compilation of observed emission line strengths from Wolf-Rayet (WR) stars, we construct evolutionary synthesis models for young starbursts. We explicitly distinguish between the various WR subtypes (WN, WC, WO), whose relative frequency is a strong function of metallicity, and we treat O and Of stars separately.

We calculate the numbers of O and WR stars produced during a starburst and provide detailed predictions of UV and optical emission line strengths for both the WR stellar lines and the major nebular hydrogen and helium emission lines, as a function of several input parameters related to the starburst episode. We also derive the theoretical frequency of WR-rich starbursts.

Our models predict that nebular He II $\lambda 4686$ emission from a low-metallicity starburst should be associated with the presence of WC/WO stars and/or hot WN stars evolving to become WC/WO stars. In addition, WR stars contribute to broad components beneath the nebular Balmer lines; the broad WR component may constitute several percent of the total flux in the line.

We review the various techniques used to derive the WR and O star content from integrated spectra, assess their accuracy, and propose two new formulae to estimate the WR/O number ratio from UV or optical spectra.

We also explore the implications of the formation of WR stars through mass transfer in close binary systems in instantaneous bursts. While the formation of WR stars through Roche lobe overflow prolongs the WR dominated phase, there are clear observational signatures which allow the phases in which WR stars are formed predominantly through the single or the binary star channels to be distinguished. In particular at low metallicities, when massive close binaries contribute significantly to the formation of

³Beatrice Watson Parent Fellow

WR stars, the binary-dominated phase is expected to occur at ages corresponding to relatively low $H\beta$ equivalent widths.

The observational features predicted by our models allow a detailed quantitative determination of the massive star population in a starburst region (particularly in so-called “WR galaxies”) from its integrated spectrum and provide a means of deriving the burst properties (e.g., duration, age) and the parameters of the initial mass function of young starbursts. The model predictions should provide the most reliable determinations to date. They can also be used to test the current theories of massive star evolution and atmospheres and investigate the variation in stellar properties with metallicity.

Subject headings: galaxies: starburst — galaxies: stellar content — H II regions — stars: Wolf-Rayet

1. Introduction

Wolf-Rayet (WR) galaxies are a subset of galaxies in which broad emission lines from WR stars are detected in the integrated galaxy spectra (Conti 1991). (A recent review of the properties of WR stars can be found in Maeder & Conti 1994.) Typically, lines of He (He II λ 4686), C (C III/C IV λ 4650, C IV λ 5808), and N (N III λ 4640) are seen. The strongest features are usually those at λ 4650-4690, whose blended emission is often referred to as the “WR bump”. The strength of the various stellar emission lines has been used to estimate the number of WR stars present in these galaxies. Typical values are in the range $N(WR) \sim 100 - 10^5$ (see e.g., Vacca & Conti 1992, hereafter referred to as VC92). Because WR stars are the short-lived descendants of the most massive stars ($M \gtrsim 35M_{\odot}$), the detection of WR emission lines in a starburst galaxy spectrum immediately places powerful constraints on several parameters characterizing the starburst episode: (1) the number of WR stars relative to the number of O stars must be large, and therefore the burst episode must have been short; (2) the initial mass function during the star formation episode must have extended to large masses (at least beyond $35 M_{\odot}$); and (3) the time elapsed since the burst ended must be less than a few Myrs. Thus, the presence of large numbers of WR stars in a starburst galaxy can be used as a signpost indicating a recent burst of massive star formation.

The first models which attempted to quantify these constraints on the WR populations in starbursts were introduced by Arnault, Kunth & Schild (1989). The comparison of their models with observations of ~ 45 extragalactic H II regions and/or galaxies with detected WR emission lines led to several important conclusions which were largely confirmed by later studies: (1) The observed decrease of the WR bump/H β intensity ratio with metallicity (Z) and the observed variations in the WR and O star populations in

the local environment are due to the same effect, namely the strong influence of Z on stellar mass loss leads to a significant decrease in the WR population at low Z (Maeder, Lequeux & Azzopardi 1980); and (2) The derived WR/O number ratio indicates that star formation must have occurred over only a short period compared to the lifetime of massive stars.

Synthesis models including more recent evolutionary tracks and predicting a large variety of observational quantities were constructed by Mas-Hesse & Kunth (1991a), and later updated by Cerviño & Mas-Hesse (1994). The WR features included in their models are the 4650 WR bump and C IV λ 5808. Mas-Hesse & Kunth (1991b, 1997) used these models to analyze the spectra of nine WR galaxies.

The use of the WR bump to determine the WR population presents several difficulties. The feature is composed of several stellar emission lines, whose strengths can vary substantially depending on the relative numbers of the various types of WR stars present. Furthermore, the stellar lines are often blended with nearby nebular emission lines of Fe, He, or Ar. Krüger et al. (1992) were the first to synthesize the separate He II and C components of the WR bump, in an attempt to circumvent the problem of nebular line contamination, and to determine the dominant WR subtype present.

The effect of varying star formation rates, initial mass function, age and metallicity on massive star populations was studied in depth by Meynet (1995), who first stressed the importance of WR stars of the WC sequence. Although the extensive models of Leitherer & Heckman (1995) include a detailed treatment of WR and O stars, observational features due to WR stars are not predicted. The same also holds for the evolutionary models of García-Vargas, Bressan & Díaz (1995).

Discoveries (usually serendipitous) of WR features in extragalactic objects have resulted from studies covering a wide range of topics, from

the primordial He abundance determination (cf. Kunth & Sargent 1983, Kunth & Joubert 1985, Izotov, Thuan & Lipovetsky 1994, 1997a; Izotov & Thuan 1997), the nature of Seyfert galaxies (Heckman et al. 1997), to starbursts in cooling flows (Allen 1995). A considerable number of new observations can be expected with the new generation of 8-10m class telescopes. To date the total number of known WR galaxies is ~ 90 37 of which were included in the first catalogue compiled by Conti (1991). However, quantitative analyses of the WR and O star content has been carried out for only few (~ 20) objects for which high quality spectra are available (see VC92, Krüger et al. 1992, Mas-Hesse & Kunth 1991b, 1997; Meynet 1995; Schaerer 1996c; Schaerer et al. 1997).

In the present paper we construct new synthesis models (building upon the models of Schaerer 1996c) tailored to the analysis of massive star populations in young starburst galaxies. Using up-to-date input physics (stellar evolution tracks, stellar atmospheres, and a new compilation of empirical WR line fluxes), we provide detailed predictions of many stellar and nebular features from the UV to the optical, most of which have not been included in previous models. By combining our new models with the observed strength of the WR emission features, as measured with medium to high spectral resolution spectra of sufficient quality (typically $S/N \gtrsim 20$), one can place constraints on the burst parameters which are stricter than those derived from earlier models. With these latest models it is possible to constrain the IMF slope (cf. Schaerer 1996c), study the WC and WN populations in starbursts (cf. Meynet 1995; Schaerer & Vacca 1996; Schaerer et al. 1997) and to address the question of the nature of nebular He II emission in extragalactic H II regions on quantitative grounds (Schaerer 1996c, Schaerer & Vacca 1996). More generally the present models can be applied to determine accurate burst parameters (age, duration, IMF etc.), and to study mas-

sive star populations in different environments and their influence on the surrounding interstellar medium.

The paper is structured as follows: The model ingredients, the input parameters, and the synthesized quantities are described in §2. In §3 we present predictions of the O star and WR stars populations, including distinct WR subtypes, and discuss the expected frequency of WR-rich starbursts. §4 summarizes issues related to the evolution of the ionizing spectrum of burst models. The predicted evolution of nebular H and He lines is discussed in §5; the evolution of WR lines is discussed in §6. In §7 we explore the effect of massive close binary systems on the formation of WR stars in young bursts. Different methods to derive the WR and O star content from integrated UV or optical spectra are presented and re-discussed in §8. In §9 we discuss applications and tests of our models and briefly sketch future prospects for studies of massive star populations in starbursts.

2. Evolutionary synthesis models

In this Section we describe the adopted model ingredients for our evolutionary synthesis models, the most important input parameters, and the synthesized quantities.

2.1. Evolutionary tracks, stellar spectra, and nebular continuum

As in the case of most synthesis models we assume that for most purposes stellar evolution can be sufficiently well described by evolution models for single stars. The single star assumption forms the basis of what we call our “standard model”. However, we also present calculations which include close massive binaries in an approximate fashion. This first order approach will allow us to investigate the uncertainties in the results of the standard model arising from the neglect of binaries.

2.1.1. *Single star evolution*

We use the recent evolutionary tracks of the Geneva group, which incorporate five different metallicities covering the range from $Z=0.001$ ($1/20 Z_{\odot}$) to $Z=0.04$ ($2 Z_{\odot}$) (see Meynet et al. 1994 and references therein). In particular, for massive stars we use the recent grids of Meynet et al. , which incorporate mass loss rates that are a factor of two higher than those adopted in previous evolutionary models. These high-mass-loss models reproduce a large number of statistical observations of massive stars, including the WR to O star ratios in regions of constant formation (Maeder & Meynet 1994) and they should therefore be most appropriate for the purposes of the present work.

Previous evolutionary synthesis models which explicitly incorporated WR stars used different evolutionary tracks. For example, the models of Cerviño & Mas-Hesse (1994) employ the Geneva tracks with standard mass loss rates, which yield smaller WR populations than the preferred high-mass-loss models. Leitherer & Heckman (1995) adopted older tracks from Maeder (1991b), for which detailed comparisons with observations are shown in Maeder (1991a). García-Vargas, Bressan & Díaz (1995) use the Padua evolutionary tracks for which no detailed comparisons regarding individual WR stars and WR populations have been published. We feel that the high-mass-loss Geneva models used in this paper should provide the most accurate predictions of the WR and O star populations in a starburst region.

2.1.2. *Evolution of close massive binaries*

It is fairly well established that at low metallicity the primary mechanism for the formation of WR stars is through mass transfer during the evolution of massive binaries, a formation channel which should produce primarily early-type WN stars (Maeder 1982, Maeder 1991a, Maeder & Meynet 1994). Using the same evolutionary tracks as adopted in this work, Maeder & Meynet

(1994) have shown that for regions of constant star formation with metallicities between $\sim 1/10 Z_{\odot}$ (SMC) and $\sim 1.75 Z_{\odot}$ (M31), both the observed ratio of the total number of WR stars to the number of O stars present (the WR/O star ratio) and the subtype distribution of WR stars (WC/WR, WNL/WR, and WNE/WR) can be well explained if a few percent of the O stars become WR stars of mainly WNE subtype *as a consequence* of Roche lobe overflow (RLOF).

To explore the implications of WR stars formed through mass transfer in massive close binaries we proceed in the following simplified manner. We adopt the recent evolutionary calculations from de Loore & Vanbeveren (1994) at different metallicities assuming an initial mass ratio of $q = 0.6$, and Case B mass transfer. The calculations of de Loore & Vanbeveren (1994) include initial primary masses from 9 to $40 M_{\odot}$ and neglect the possibility of subsequent WR formation of the secondary. Primaries with initial masses $M_1 \gtrsim 40\text{-}50 M_{\odot}$ should in general avoid Roche lobe overflow (RLOF) (cf. Vanbeveren 1995); even if they do indeed experience RLOF their evolution should be nearly indistinguishable from that of single stars (Langer 1995). For initial masses $M_{\text{ini}} \lesssim 9 M_{\odot}$ the formation of WR stars is not expected. Since the calculations of de Loore & Vanbeveren (1994) are not available at exactly the same metallicities as the single star models, we used the tracks with metallicities closest to those for the single star models. (We adopted their solar metallicity models for $Z \geq 0.02$, their LMC models for $Z = 0.008$, and their SMC models for $Z \leq 0.004$).

Our primary goal is to derive, as a function of the age of the burst, the *total number of WR stars* (and their subtype distribution) formed from mass transfer in binary systems. For this purpose it is necessary to determine for each initial mass, whether or not at the given burst age the primary has already experienced RLOF leading to WR formation, and if it has, what the resulting WR subtype is. This is done in a

straightforward manner from the lifetimes in the WR phases as given by de Loore & Vanbeveren (1994)².

One additional parameter f is required to derive the total number of WR stars formed through the binary channel, where f is the initial fraction of stars that are primaries in close binary systems (described by the parameters given above) and will thus experience RLOF during their evolution. Because the range in initial masses covered by the binary models corresponds to zero-age main sequence (ZAMS) O stars, our definition of f turns out to be essentially identical to the one given by Vanbeveren (1995). In contrast Maeder & Meynet (1994) use $\Psi = \text{WR}_{\text{cb}}/\text{O}$, which represents the fraction of O stars which become WR stars through RLOF. Note that both definitions implicitly neglect the evolution of the secondary, which would in principle affect the number of both O and WR stars. In the case of a constant star formation rate Ψ and f are related by

$$\begin{aligned} \Psi &\approx f [t(\text{WR}_{\text{cb}})/t(\text{O}_{\text{cb}})]' \\ &= f \frac{\int_{M_{\text{min}}}^{M_{\text{max}}} t(\text{WR}_{\text{cb}})/t(\text{O}_{\text{cb}})\Phi(M)dM}{\int_{M_{\text{min}}}^{M_{\text{max}}} \Phi(M)dM}, \end{aligned} \quad (1)$$

where $t(\text{WR}_{\text{cb}})$ and $t(\text{O}_{\text{cb}})$ are the lifetimes of the primary of initial mass M in the WR phase and in the preceding O star phase, respectively. $\Phi(M)$ is the initial mass function, and M_{min} and M_{max} are the minimum and maximum initial mass of primary stars leading to WR for-

²We note that the H-burning lifetimes t_{H} from de Loore & Vanbeveren (1994, Table 1) are larger (typically by $\sim 20\%$) than those from the single star models used here. The O star lifetimes given in Vanbeveren (1995) agree, however, with those of standard evolutionary models (Schaller et al. 1992). To obtain a more consistent time for the onset of Case B Roche lobe overflow we therefore adopt the t_{H} lifetimes from Meynet et al. This leads to an earlier appearance (~ 1 Myr) of WR stars formed from mass transfer than would be obtained by using the lifetimes from de Loore & Vanbeveren. The duration of the binary WR phases are taken directly from de Loore & Vanbeveren (Table 1).

mation by RLOF. To first order the models of Vanbeveren (1995) give mass-independent values for $t(\text{WR}_{\text{cb}})/t(\text{O}_{\text{cb}})$ on the order of 0.2 and 0.1 for $Z=0.02$ and $Z \leq 0.01$ (see his Figs. 2a-4a), and hence $\Psi \approx (0.2 - 0.1) \times f$.

For numerical comparisons with Vanbeveren (1995) the standard mass loss tracks are the most appropriate. As Fig. 12 of Maeder & Meynet (1994) shows, the value of Ψ required to reproduce the observed WR/O number ratio ($\Psi \sim 0.08$ to 0.01 for $Z \leq 0.02$) is fully compatible with the values of f advocated by Vanbeveren (1995). Yet another definition of the fraction of massive close binaries is adopted in the detailed models of Vanbeveren, Van Bever & de Donder (1997). From their Table 1 (solar metallicity models using observational constraints) one can, however, easily derive the values resulting for Ψ . One finds $\Psi \sim 0.06$ - 0.08 , as expected for standard evolutionary models (see Maeder & Meynet, Fig. 12). This indicates that the assumed binary frequency of Vanbeveren, Van Bever & De Donder is in agreement with the work of Maeder & Meynet (1994). From the comparison between the theoretical and observed WR/O ratio in regions of constant star formation using the high mass loss tracks (Fig. 11 of Maeder & Meynet 1994) and the approximate (metallicity dependent) conversion of Ψ to f (see above) one obtains $f \sim 0.1$ to 0.25 for $Z=0.002$ to 0.02 . For the calculations presented here we adopt $f = 0.2$.

Knowing the number of WR stars formed by mass transfer, we now proceed to derive their impact on the most important observable quantities, i.e. on nebular recombination lines and on the emission in the broad WR features. To this end one only requires a knowledge of the ionizing flux and the number of WR stars in the different WR phases (cf. § 2.2.1). We adopt an average Lyman continuum flux of $Q_0(\text{WR}) = 10^{49}$ photons s^{-1} , independently of the WR subtype. This value roughly corresponds to the average contribution of (single) WR stars derived from burst models at the time (~ 5 Myr) where

binary stars are first expected to be formed (cf. Fig. A6). As a comparison the value used by VC92 is $Q_0(\text{WR}) = 1.7 \times 10^{49}$. The contribution of the ionizing flux in particular affects the H recombination lines, which are generally used as a reference for relative line intensity measurements. The broad WR line emission is treated as for single stars (see § 2.2.1). Since no information is available on the WC subtype from the binary models they are assigned the WC4 subtype corresponding to the dominant subtype at low Z where the role of binaries is of largest importance.

Our procedure completely neglects the detailed evolution of the binary stars in the H-R diagram. Except for the Lyman continuum, we neglect the continuum flux contribution of primaries in close binary systems, which affects only the predicted equivalent widths. This assumption is reasonable as long as the UV and optical continuum fluxes are dominated by single stars or stars in wide binary systems. The secondaries are assumed to evolve as single stars. The expected increase of their Lyman continuum flux after mass transfer (due to possible “rejuvenation”) can be neglected since the primary WR star will dominate the EUV output. We feel that this approach is a reasonable first order approximation to study the effect of WR formation through the binary channel on a stellar population. For more detailed studies the number of new parameters (mass ratio distribution, initial binary separation and more; see e.g. Dalton & Sarazin 1995, Vanbeveren, Van Bever & De Donder 1997) is large and several uncertainties associated with binary evolution (mass loss during Roche lobe overflow, mixing of secondary etc.; see e.g. Vanbeveren, Van Bever & De Donder 1997, Braun & Langer 1995) should be taken into account. Population synthesis models which include binaries and are applicable to WR galaxies have also been presented by Cerviño & Mas-Hesse (1996), Cerviño, Mas-Hesse & Kunth (1996) and Vanbeveren, Van Bever & De Donder (1997). First results from

our work have been reported in Schaerer & Vacca (1996).

2.1.3. Emergent fluxes

To describe the spectral evolution we rely on three different sets of theoretical models:

1) For the main sequence evolution of massive stars we use the spectra produced by the combined stellar structure and atmosphere (*CoStar*) models of Schaerer et al. (1996a, b) and Schaerer & de Koter (1996). The models, which include non-LTE effects, line blanketing, and stellar winds, cover the entire parameter space of O stars. As shown by Schaerer (1996b) and Schaerer & de Koter (1997) they represent significant improvements over previous calculations, particularly for the ionizing fluxes. In practice we use the model set given by Schaerer & de Koter (1997) for stars with initial masses $M_{\text{ini}} \geq 20 M_{\odot}$. Additionally we restrict the use of these models to the following $T_{\text{eff}}\text{-log } g$ domain: $\log g \geq 2.2$ and $\log g < 5.71 \times \log T_{\text{eff}} - 21.95$. The latter restriction corresponds roughly to an O9/B0 spectral type. This parameter range spans the domain of validity of the models and yields ionizing fluxes which merge smoothly with those calculated from the Kurucz (1992) models described below. For solar metallicity we consistently use the corresponding *CoStar* models. At subsolar metallicities we adopt the low metallicity ($Z = 0.004$) calculations of Schaerer & de Koter. For $Z = 0.04$ we use a new set of *CoStar* models (Schaerer 1996, unpublished).

2) For stars less massive than $20 M_{\odot}$ we use the line-blanketed plane-parallel LTE atmosphere models of Kurucz (1992) calculated with a microturbulent velocity of $v_{\text{turb}} = 2 \text{ km s}^{-1}$. The Kurucz models cover a large range of metallicities, characterized by the iron abundance $[\text{Fe}/\text{H}]$. For each set of evolutionary tracks (characterized by a particular value of the total metal abundance Z) we adopted the Kurucz model atmospheres with the corresponding value of $[\text{Fe}/\text{H}]$. The assignments for the specific metallicities considered in this pa-

per (dictated by the metallicities of the evolutionary tracks) were as follows: we used the Kurucz models with $[\text{Fe}/\text{H}] = -1.5$ for $Z = 0.001$; $[\text{Fe}/\text{H}] = -1$ for $Z = 0.004$, $[\text{Fe}/\text{H}] = -0.5$ for $Z = 0.008$, $[\text{Fe}/\text{H}] = 0$ for $Z = 0.020$, and $[\text{Fe}/\text{H}] = +0.3$ for $Z = 0.040$. More accurate assignments are not necessary since the variations of the stellar spectra with metallicity are much less important than those due to changes of the evolutionary tracks.

3) Stars in the WR phases are described by the spherically expanding non-LTE models of Schmutz, Leitherer & Gruenwald (1992). We identify the core radii and core temperatures of their models with the radius and T_{eff} from the wind-free hydrostatic stellar model (see Schaerer 1996a for distinction and a discussion). Test calculations using the subphotospheric radii of Schaerer (1996a) yield essentially identical results. The additional parameters which control the emergent spectrum of WR stars are the mass loss rate \dot{M} (taken from the stellar evolution models) and the terminal velocity v_{∞} of the wind. For WN and WC stars we use the fitting formulae from Schaerer (1996a, Eqs. 8 and 9), which account for the strong dependence of v_{∞} on the WR subtype. For WO stars we adopt $v_{\infty} = 4000 \text{ km s}^{-1}$, the average value of WO3 and WO4 stars (Kingsburgh & Barlow 1995, Kingsburgh, Barlow & Storey 1995). It should be noted that the atmosphere models of Schmutz, Leitherer & Gruenwald (1992) used here include only He and do not account for variations in the emergent spectra due to possible composition or metallicity effects. These authors argue that uncertainties in the hydrodynamic structure should have larger effects than the neglect of metals. For WN stars, pilot studies carried out by Schmutz (1991) indicate that the effects of line blanketing in WR atmospheres produce moderate changes in the predicted spectra, although Crowther et al. (1997) find a significant reduction of the ionizing flux for a line-blanketed WNL model. For WC/WO stars models which incorporate the abundant species of C and O (cf.

Gräfener et al. 1997) have just been developed. Once line-blanketed atmosphere models for WR stars have matured and become widely available, they will be incorporated in our synthesis routines.

In addition to the stellar continuum, we have included the nebular continuum spectrum in our models. As first shown by Huchra (1977) the nebular contribution becomes important when hot stars providing a large number of ionizing photons are present. To treat the nebular emission in a simplified way we assumed the emitting gas has an electron temperature $T_e = 10000 \text{ K}$, an electron density $N_e = 100 \text{ cm}^{-3}$, and a helium abundance of 10 % by number relative to hydrogen. The monochromatic luminosity of the gas, which is proportional to the number of Lyman continuum photons Q_0 , is given by

$$L_{\lambda} = \frac{c}{\lambda^2} \frac{\gamma_{\text{total}}}{\alpha_B} f_{\gamma} Q_0, \quad (2)$$

where α_B is the case B recombination coefficient for hydrogen, and f_{γ} is the fraction of ionizing photons absorbed by the gas. For the continuous emission coefficient γ_{total} we used the atomic data from the tables of Aller (1984) and Ferland (1980) for the wavelength regimes shortward and longward of $1 \mu\text{m}$, respectively, to account for free-free and free-bound emission by hydrogen and neutral helium, as well as for the two-photon continuum of hydrogen³.

2.2. Input parameters

Evolutionary synthesis consists of calculating the properties of an entire stellar population as a function of time. In this work we concentrate on the time evolution of young populations experiencing star formation on timescales short compared to the evolutionary timescales of massive stars. As an idealized case we assume an instantaneous burst occurring at time $t = 0$. The time

³We ignore two-photon continuum emission for $\lambda > 1 \mu\text{m}$ and assume $\gamma_{\text{HeI}} = \gamma_{\text{H}}$.

evolution of the burst is followed by isochrone synthesis based on a subroutine kindly provided by Georges Meynet.

The parameters defining the burst population are the following: the initial metallicity Z , the initial mass function (IMF), and the total mass of stars formed in the burst. The last parameter serves only as a normalization constant and is not relevant for the quantities discussed in this work.

For the IMF we adopt a power law $\phi(m) = dN/dm \propto m^{-\alpha}$ between the upper and low cut-off masses, M_{up} and M_{low} respectively. The IMFs in massive-star forming regions in the Local Group generally have slopes (α) between 2 and 2.8 (see e.g., Maeder & Conti 1994; Massey et al. 1995b), in agreement with the Salpeter (1955) value of $\alpha = 2.35$. We adopted the Salpeter IMF for our “standard” model. For the quantities and burst ages analyzed in this work the influence of the lower mass cut-off is negligible, and we use $M_{\text{low}} = 0.8 M_{\odot}$. A large number of observations indicate that the most massive stars have masses of the order of $100 M_{\odot}$ or larger (e.g. Kudritzki 1996). We adopt $M_{\text{up}} = 120 M_{\odot}$ for all calculations. For an accurate description of the evolutionary status of stars close to the lower mass limit for WR formation, M_{WR} , we use the tabulated values from Maeder & Meynet (1994).

Results from calculations using variations of the “standard” input parameters are not presented here, but are available in electronic format (see Appendix).

2.2.1. WR emission lines

To predict the broad stellar emission lines we have compiled average line fluxes for Of, WNE, WNL, WC, and WO stars. Our compilation, given in Tables 1 and 2, includes the strongest emission lines of H, He, C, and N in the UV and optical spectral ranges: He II $\lambda 1640$, the N III/V $\lambda 4640$ blend, C III/IV $\lambda 4650$, He II $\lambda 4686$, the He II $\lambda 4861 + \text{H}\beta$ blend (denoted as 4861), the

He II+C IV $\lambda 5411$ blend, C III $\lambda 5696$, the C IV $\lambda \lambda 5808-5812$ multiplet (denoted as 5808), and the He II $\lambda 6562 + \text{H}\alpha$ blend (denoted as 6560). All other optical emission lines from WR stars are expected to be much weaker, and therefore have not been included in our model calculations. For comparison with previous models we also synthesize the two broad “WR bumps” (the N III/V+C III/IV+He II blend at $\lambda \sim 4650$, and C IV $\lambda 5808$). The calibration from Smith (1991) of these features is reported in Table 3 for completeness.

For Of and WN stars we use the absolute flux in He II $\lambda 4686$ (col. 9 of Table 1) as a reference and compute line strength ratios for all other lines relative to this reference. For WC and WO stars we use C IV $\lambda 5808$ (col. 10 of Table 2) as the line strength reference. All line fluxes are expressed in terms of these “reference lines”.

Of stars: The strongest emission lines in Of stars are He II 4686 and the N III/V 4640 blend. The He II/N III ratio shows considerable variations between individual OIf stars. We adopted a ratio of $L(4640)/L(4686) = 0.1$, which should strictly be considered a lower limit. For the He II 4686 line we adopted an average luminosity determined from one O3If/WN6 and one O6Iaf star in the LMC (Crowther 1996, private communication). This yields a value of $2.5 \times 10^{35} \text{ erg s}^{-1}$. This is a factor 2.6 lower than the line flux from

Table 3: Average “WR bump” line luminosities for WN and WC stars. Logarithm of line luminosities in ergs^{-1} . From Smith (1991, LMC stars)

	C III/IV4650+He II4686	C IV5808
WN7	36.5	35.1
WC4	36.7	36.5

Table 1: Adopted line luminosities for broad stellar emission lines from WN stars. Mean absolute line luminosities are given for the reference line He II 4686 in erg s^{-1} for each subtype. Mean fluxes ratios with respect to this reference line are given for the other lines. Below each mean value are the standard deviation and the number of stars included in the mean.

Subtype		$\frac{1640}{4686}$	$\frac{4640}{4686}$	$\frac{4861}{4686}$	$\frac{5411}{4686}$	$\frac{5808}{4686}$	$\frac{6560}{4686}$	4686
WNE	Mean	7.95	...	0.129	0.137	0.074	0.202	5.2×10^{35}
	σ	2.47	...	0.031	0.022	0.027	0.130	2.7×10^{35}
	N	28	...	7	38	5	7	26
WNL	Mean	7.55	0.244/0.616 ^a	0.309	0.107	0.062	1.596	1.6×10^{36}
	σ	3.52	0.151/0.519	0.107	0.022	0.036	1.511	1.5×10^{36}
	N	17	5/7	11	30	10	4	19

^a The first set of values for N III 4640 were derived from LMC WNL stars and were used for models with $Z < Z_{\odot}$; the second set of values were derived from Galactic WNL stars and were used for models with $Z \geq Z_{\odot}$.

the four O3f/WN stars in R136a recently analyzed by de Koter, Heap & Hubeny (1997); for those stars $L(4686) = 6.5 \times 10^{35} \text{ erg s}^{-1}$ (de Koter 1996, private communication). As can be seen the line luminosity of the R136a stars is compatible with the average value derived for WNE stars.

WN stars: Unfortunately, there is no single reference that provides intrinsic fluxes for all the lines in WN spectra that we wish to include in our models. We compiled flux measurements from the studies of Morris (1995) and Smith, Shara, & Moffat (1996, hereafter SSM96). Although Morris (1995) and SSM96 present results for many of the same stars, the two sets of measurements have only two lines in common: He II $\lambda 4686$ and He II $\lambda 5411$. We used the 5411/4686 line ratio and the absolute value of the 4686 flux to check that the two sets of measurements were consistent.

We began by dereddening the observed fluxes for the Galactic stars in both samples with the color excess values given by Morris et al. (1993), with the revisions given by Morris (1995). For three stars for which values of $E(B - V)$ were not given we adopted the values given by Hamann et al. (1993). We used the reddening curve given by Seaton (1979) and $R_V = 3.2$. For the LMC stars we used the extinction curve given by Seaton (1979) for the Galactic foreground reddening and the average LMC extinction curve derived by Vacca (1992; see also Morris et al. 1993) with $R_V = 3.2$ for the reddening within the LMC. We assumed a maximum foreground reddening value of $E(B - V)_{fg} = 0.03 \text{ mag}$.

We adopted the subtype classifications given by SSM96. This rarely resulted in a change of more than one subtype with respect to older classifications (e.g., Conti & Massey 1989). We then divided the sample into WNE and WNL subclasses. The WNE subclass consists of stars

Table 2: Adopted line luminosities for broad stellar emission lines from WC/WO stars. Mean absolute line luminosities are given for the reference line C IV 5808 in erg s^{-1} for each subtype. Mean fluxes ratios with respect to this reference line are given for the other lines. Below each mean value are the standard deviation and the number of stars included in the mean.

Subtype		$\frac{1640}{5808}$	$\frac{4650}{5808}$	$\frac{4686}{5808}$	$\frac{4861}{5808}$	$\frac{5411}{5808}$	$\frac{5696}{5808}$	$\frac{6560}{5808}$	5808
WO	Mean	2.65	0.51	0.386	...	0.026	...	0.078	1.1×10^{36}
	σ	1.44	0.18	0.158	...	0.012	...	0.065	0.2×10^{36}
	N	2	3	3	...	3	...	2	3
WC4	Mean	2.14	1.71	...	0.019	0.023	0.021	0.045	3.0×10^{36}
	σ	1.09	0.53	...	0.009	0.009	0.018	0.014	1.1×10^{36}
	N	16	23	...	11	14	11	19	18
WC5	Mean	5.14	2.53	...	0.022	0.036	0.077	0.074	9.8×10^{35}
	σ	4.43	0.49	...	0.013	0.018	0.033	0.011	2.3×10^{35}
	N	5	9	...	7	8	9	8	2
WC6	Mean	7.60	2.98	...	0.047	0.054	0.184	0.112	8.9×10^{35}
	σ	6.17	0.52	...	0.012	0.006	0.083	0.037	1.9×10^{35}
	N	6	10	...	9	9	10	10	3
WC7	Mean	10.22	3.21	...	0.069	0.076	0.579	0.177	1.4×10^{36}
	σ	5.25	0.49	...	0.024	0.027	0.214	0.028	0.6×10^{36}
	N	10	15	...	13	14	15	14	4
WC8	Mean	13.69	3.30	...	0.096	0.091	1.968	0.580	3.5×10^{35}
	σ	14.58	0.45	...	0.037	0.031	0.649	0.284	3.1×10^{35}
	N	5	7	...	5	6	7	8	3
WC9	Mean	4.47	4.46	...	0.294	0.135	3.705	1.243	2.0×10^{35}
	σ	1.25	0.97	...	0.095	0.033	0.514	0.256	2.0×10^{35}
	N	3	17	...	17	17	18	16	2

with subtypes between WN2 and WN4, while the WNL subclass consists of stars with subtypes between WN6 and WN9. This division agrees with the definitions and assignments given by Conti & Massey (1989). Consistent subclass identifications could not be assigned to the WN5 subtype and these stars were excluded from the averages. We then computed the average dereddened 5411/4686 ratios for LMC and Galactic stars for the two subclasses in each sample. It was found that the averages for the Morris sample and those for the SSM96 sample could be brought into agreement only if stars with low hydrogen abundances (WNb and WNo stars, as classified by SSM96) were excluded from the WNL averages. WR 43 was the only exception to this rule of excluding objects classified by SSM96 as having low H abundance from the WNL averages; although SSM96 classify this object as a WN6o, Drissen et al. (1995; see also Dessart & Crowther 1997) find that it is composed of three WN6h stars. Correspondingly, we excluded those stars containing a substantial amount of hydrogen (WNh or WN(h) stars, again as classified by SSM96) from the WNE averages. Once the mean line ratios were found to be consistent between the two samples, we combined the samples. The flux ratios of He II λ 1640/He II λ 4686 and He II λ 5411/He II λ 4686 are taken from Morris (1995), while the other line strength ratios are taken from SSM96.

As shown by SSM96 the strength of the N λ 4640 line depends on the initial abundance of the progenitor star. For solar metallicities and larger we adopt the Galactic average, while for $Z < Z_{\odot}$ we adopt the lower LMC value. For all of the other line ratios, we derived average values by combining the LMC and Galactic stellar samples, after confirming that the means of the two samples for each line ratio were in agreement. We excluded from the averages any values which were found to be more than 3σ away from the mean; the averages were then re-computed with the smaller sample. This process resulted in the exclusion of only a few individual line flux values

from the calculations of the various means.

The absolute luminosity of He II for each subclass was derived from the Morris (1995) sample of LMC stars and those Galactic stars that are definite or probable members of cluster or associations with reliable distance estimates. We assumed a distance of 50.1 kpc (DM=18.50) for the LMC; distances for stars in Galactic clusters or associations were taken from Lundström & Stenholm (1984), with revisions given by Moffat (1983; for NGC 3603), Garmany & Stencel (1992), Smith, Meynet, & Mermilliod (1994), and Massey, Johnson, & DeGioia-Eastwood (1995a) and references therein. For WR 43/NGC 3603, we divided the total dereddened flux measured by Morris (1993) into three components, with relative contributions in agreement with the line measurements of Drissen (1997, private communication). The resulting mean WN line luminosities and line ratios, as well as the standard deviations about the mean and the number of stars included in each mean, are presented in Table (1).

A comparison of the line fluxes determined for individual stars by Morris (1995) with those measured by Crowther (1997, private communication) and Crowther & Dessart (1997) on substantially higher resolution spectra reveals a systematic difference of $\sim 20 - 30\%$ (in the sense that the line fluxes from Morris 1995 are larger than those of Crowther & Dessart 1997). It is not completely clear what the cause of this discrepancy might be, but if we assume that the higher resolution spectra yield more accurate line fluxes, then we conclude that our adopted line luminosities may be $\sim 30\%$ too large. In addition, the absolute luminosity of He II λ 4686 exhibits substantial variations within the WNL subclass, and a mean luminosity for this line is rather uncertain. The situation is illustrated in Fig. A1, in which we plot the line luminosities from Crowther (1997) and Crowther & Dessart (1997) against the bolometric luminosities derived by these authors from their spectral analy-

ses. The large variation in line luminosity within the WNL subclass is easily seen. The figure also reveals that there may be a difference in the line luminosity between stars with $L < 10^6 L_\odot$ and those with $L > 10^6 L_\odot$. The lower luminosity stars (in the combined Galactic plus LMC sample) have a mean He II 4686 line luminosity of $5.6 \times 10^{35} \text{ erg s}^{-1}$, while the higher luminosity stars have a mean line luminosity of $3.1 \times 10^{36} \text{ erg s}^{-1}$. However, the uncertainties in the mean values for these two luminosity classes are also very large, and we have chosen to use a constant line luminosity for all bolometric luminosities of WNL stars in our models. The entire WNL sample from Crowther (1997) has a mean line luminosity of $1.1 \times 10^{36} \text{ erg s}^{-1}$, which agrees well with our adopted value after the systematic differences between the Crowther (1997) and Morris (1995) line flux measurements are taken into account.

Despite the uncertainties in the mean luminosity of the He II 4686 line, our estimate of $1.6 \times 10^{36} \text{ erg s}^{-1}$ is in excellent agreement with the value of $1.7 \times 10^{36} \text{ erg s}^{-1}$ determined by Vacca (1992; see also VC92). Vacca (1992) demonstrated that this value, when combined with spatially-integrated line flux measurements, yields an estimate for the number of WNL stars within the 30 Doradus complex that is in good agreement with the number derived by directly counting objects with spectroscopic identifications. Furthermore, Terlevich et al. (1996) used this mean luminosity value to determine the number of WN stars in NGC 604 from their spatially-integrated spectra. They found that their estimate was again in excellent agreement with the number of WR stars found by Drissen, Moffat, & Shara (1993) using narrow-band *HST* images. In addition, Crowther & Dessart (1997) find that this value of the mean line luminosity yields a number for the WNL stars within the NGC 3603 complex that is in good agreement with the observed number (Drissen et al. 1995). Unfortunately, additional tests of our value are currently not available.

To reduce the uncertainties of the WR line strengths used in the present models it would be highly desirable to understand the observed large variations of the line luminosities (Fig. 1) and their dependence on stellar parameters. If correlations of the line strengths with physical parameters can be established, these can be used in future models to provide a more accurate picture of the WR populations. It is also necessary to clarify the relationship between WR classifications and stellar models (cf. Smith & Maeder, 1997). For example, the WNE and WNL classifications we have adopted are defined according to purely phenomenological criteria and do not necessarily correspond directly to the definitions employed in the stellar evolutionary models. Our additional separation of the stellar sample into objects with and without hydrogen represents a compromise between the observational definitions of WNE and WNL stars and those employed by the evolutionary models. With these criteria we have attempted to link the observations and models as closely as possible. The adopted approach should yield average line luminosities and ratios that are representative of the properties of the classes of hydrogen-free and hydrogen-rich WN stars.

WC and WO stars: In view of the substantial variations in the frequency distributions of WC/WO subtypes with environment (cf. Smith & Maeder 1991), as well as the strong variations in spectral signatures with subtype, we chose to treat the various WC subtypes separately. The assignment of the WC/WO subtype from the evolutionary model is discussed below (§2.3).

The task of compiling dereddened line fluxes was substantially easier in the case of WC and WO stars. Average line fluxes of WC stars have been derived by Smith, Shara, & Moffat (1990a, b, hereafter SSM90a, SSM90b) and recently by Brownsberger (1995), who provided an extensive list of dereddened line fluxes for nearly every known WC star in the Galaxy and the LMC. Their results agree within their quoted uncertainties. We adopted the dereddened line fluxes

presented by Brownsberger (1995) and computed average values of the line flux ratios (relative to the strength of C IV $\lambda 5808$) as a function of WC subtype; the subtypes were assigned according to the classification scheme of SSM90a and SSM90b. (The method used by Brownsberger to compute the reddening for each star and deredden the line fluxes is identical to the method we adopted for WN stars; see above.) The average luminosity in C IV $\lambda 5808$ for each subtype was determined from WC stars in the LMC and those Galactic stars located in clusters or OB associations for which reliable distances could be determined. Distances were taken from Lundström & Stenholm (1984), with revisions given by Garmany & Stencel (1992), Smith, Meynet, & Mermilliod (1994), and Massey, Johnson, & DeGioia-Eastwood (1995a) and references therein. Unfortunately it is not possible to check for consistency in the C IV line luminosity between LMC and Galactic WC stars; the LMC contains only one WC star with a subtype later than WC4, and there are no WC4 stars in the Galaxy with well determined distances. For the WC4 subtype we adopted the average C IV $\lambda 5808$ luminosity of the LMC stars. This value is 0.5 dex larger than that found for WC5-7 stars in the Galaxy, which agrees with the findings of SSM90b. The mean line ratios were derived by combining the LMC and Galactic WC4 samples, after confirming that their individual mean values were completely consistent with one another. For all other types, we adopted the mean line luminosity and line ratios derived from the Galactic stars. The average line luminosities and ratios, as well as the standard deviations about the means and the number of stars included in the estimation of the means, are given for each subtype in Table 2. The averages were computed iteratively, as described above for the WN stars, by excluding those individual values that were found to be more than 3 σ from the means. This resulted in the exclusion of only a few line flux values from the calculations of the various means.

The emission of WC stars in the 4650 bump requires an additional comment. The broad C III/C IV $\lambda 4650$ blend also includes the contribution from He II $\lambda 4686$, which usually can not be separated. From SSM90b (their Table 2) we find that for WC5-9 stars He II 4686 contributes on the average $\sim 12\%$ to the 4650 blend; SSM90a estimate He II 4686 contributes 8 to 30 % of the blend for WC4. We include the strength of the entire 4650 blend in our models and do not treat the He II 4686 emission from WC stars separately.

For WO stars we have derived average line luminosities from the dereddened line flux measurements of three WO3 and WO4 stars given by Kingsburgh & Barlow (1995) and Kingsburgh, Barlow & Storey (1995). While the line luminosities of these objects (all located in low metallicity environments: LMC, SMC, IC1613) exhibit relatively little scatter, they are systematically stronger than the line luminosities for the two known galactic WO1 and WO2 stars. This difference may be attributed to differences in their evolution (Kingsburgh, Barlow & Storey, 1995). Since WO stars are expected to occur mainly at low metallicities (cf. § 3.2) it seems justified to adopt the properties of only WO3/WO4 stars. We used the fractional line contributions provided by Kingsburgh, Barlow & Storey (1995) and Kingsburgh & Barlow (1995) to decompose the total flux in the emission blend at 4650 Å into the flux from C IV $\lambda 4658$ and that from the component due to C IV $\lambda 4685$, and He II $\lambda 4686$. (The latter two lines would not usually be separable in the spectra of W-R galaxies.) From test calculations we find that other emission lines which are prominent only in the rare WO stars are predicted to be very weak and are therefore not included in our models. For completeness we list their average line luminosities, which are: $L(\text{O IV } \lambda 3400) = 1.9 \times 10^{36} \text{ erg s}^{-1}$, $L(\text{O VI } \lambda 3811) = 1.5 \times 10^{36} \text{ erg s}^{-1}$, and $L(\text{O V } \lambda 5590) = 1.5 \times 10^{35} \text{ erg s}^{-1}$. Note that we have adopted a distance of 58.9 kpc for the SMC and

661 kpc for IC 1613.

2.3. Synthesized quantities

The most important synthesized quantities can be classified in three groups: population statistics, nebular quantities, and WR emission lines.

2.3.1. Population statistics

For comparisons with star counts it is useful to derive the numbers of stars with different spectral types. Of particular interest for young bursts is the number of O stars, the total number of WR stars and their distribution among the WNL, WNE, and WC/WO subclasses. WR stars and the various WR subclasses are defined by their surface abundances and their effective temperature from the evolutionary models (see e.g. Maeder 1991b). Hydrogen-free WN models are considered to be WNEs, while those containing hydrogen are treated as WNLs. We also estimate the number of stars belonging to the various WC subtypes (WC4 - WC9) and WO subclasses (cf. below); the frequency distribution among these subtypes depends strongly on metallicity (e.g. Smith & Maeder, 1991). We assign WC and WO subtypes according to their surface abundance, i.e. by the (C+O)/He number ratio.⁴ Note that in some cases the WR phase can be entered during the core H-burning phase (cf. Meynet et al. 1994). We define O-type

⁴WC/WO subtypes are assigned as follows: WC9: (C+O)/He \leq 0.08, WC8: (C+O)/He \in (0.08,0.15], WC7: (C+O)/He \in (0.15,0.25], WC6: (C+O)/He \in (0.25,0.35], WC5: (C+O)/He \in (0.35,0.43], WC4: (C+O)/He \in (0.43,1.], WO: (C+O)/He $>$ 1. Here the values of Smith & Maeder (1991) have been adjusted slightly to account for the recent C, O, and He determinations in WC4 stars by Gräfener et al. (1997). The correspondence between spectral types and C, O abundance is not completely agreed upon, however (cf. e.g. Eenens & Williams 1992 and Koesterke & Hamann 1995). More detailed analyses, covering a large range of WC subtypes and including oxygen abundance determinations, will be necessary to assess the validity of the correlation of (C+O)/He with WC subtype.

stars to be those H-burning objects with effective temperatures $T_{\text{eff}} > 33000$ K.

We also estimate the number of Of stars and include the contribution of their stellar emission lines to the observed emission features. We assumed that all O stars with surface gravities below the average value found for OIa stars can be counted as Of stars. We used the recent calibration of Vacca et al. (1996) to derive $\log g$ as a function of T_{eff} for the O Ia luminosity class. For consistency we adopt the calibration given for the gravity g_{evol} determined from evolutionary models (following Vacca et al. 1996).

2.3.2. Nebular quantities

We synthesize the following H and He nebular recombination lines under the assumption of Case B recombination: H α , H β , He I λ 4471, and He II λ 4686. The adopted electron temperature and density are the same as given above. The emissivities and recombination coefficients are taken from Osterbrock (1989). The luminosity emitted in the emission lines is calculated from the number of Lyman, He I, and He II photons (Q_0 , Q_1 , and Q_2 respectively) using the relations

$$L(\text{H}\alpha) = 1.36 \times 10^{-12} f_{\gamma} Q_0 \quad (3)$$

$$L(\text{H}\beta) = 4.76 \times 10^{-13} f_{\gamma} Q_0 \quad (4)$$

$$L(4471) = 2.22 \times 10^{-13} f_{\gamma} Q_1 \quad (5)$$

$$L(4686) = 1.02 \times 10^{-12} f_{\gamma} Q_2 \quad (6)$$

where L is given in [erg s^{-1}] and Q_i in [s^{-1}]. f_{γ} is the fraction of ionizing photons absorbed by the gas. A fraction $(1 - f_{\gamma})$ is assumed to escape the system. Our “standard” model assumes an ionization bounded nebula with $f_{\gamma} = 1$. It should be noted that the strength of He I λ 4471 predicted from Eq. 6 above will be incorrect when there are enough photons above 24.6 eV to fully ionize helium in the nebula; this situation corresponds approximately to equivalent effective temperatures of $T_{\text{eff}} > 40000$ K.

2.3.3. WR emission lines

Several observational signatures of WR stars in the integrated spectrum of a starburst region are computed according to the prescriptions given in Sect. 2.2.1.

3. Wolf-Rayet and O star populations in young starburst

We now discuss the model predictions regarding the massive star populations. We present the time evolution of the WR and O star populations for an instantaneous burst at different metallicities. We explicitly consider the various WR subtypes (primarily WNL and WC/WO) and estimate the fraction of O stars which exhibit emission lines (Of stars). The results presented here are essential for understanding the behaviour of the synthesized spectral lines and other observable features which will be discussed in § 5 and 6.

In Figure A2 we show the time evolution of the stellar number ratios $WR/(WR+O)$, $WNL/(WR+O)$, and $WC/(WR+O)$, as well as the Of/O ratio for the five metallicities between $Z=0.001$ and 0.040 . (Note that here WC stands for WC and WO stars, irrespective of the distinction made between these types in the calculation of the line strengths.) The values were calculated for an instantaneous burst (occurring at $t = 0$) and a Salpeter IMF. Variations in the relative WR and O star populations with other parameters (IMF slope, upper mass limit, star formation rate and different evolutionary tracks) have been discussed in detail by Meynet (1995), and therefore will not be repeated here. Nevertheless, we must comment on a small discrepancy between our results for WR populations and those presented by Meynet (1995). The differences in the two sets of results can be seen by comparing, for example, our predictions for the WC population at $Z=0.004$ (Fig. A2) with those presented in Fig. 3 from Meynet (1995). As Fig. A2 shows, we predict a strong decrease of the WC population after

~ 4 Myr, while in models of Meynet (1995) the WC population remains dominant until the end of the WR-rich phase ($t \sim 5.2$ Myr). The origin of this discrepancy resides in the use of different techniques to interpolate between the two (discrete) evolutionary tracks above and below the mass limit of WR formation (in the case of $Z=0.004$, between the 60 and $40 M_{\odot}$ track). This discrepancy occurs therefore only for ages larger than the lifetime of the least massive star whose initial mass is larger the WR mass limit ($60 M_{\odot}$ in the present case). While Meynet (1995) performs a linear interpolation on the lifetimes in the various WR phases (WNL, WNE, and WC) as a function of initial mass between those two tracks, our classification of WR subtype is based on an interpolation of the surface abundances on the isochrone. Meynet's method predicts the existence of WC stars until the end of the WR phase, while in our case models close to the WR mass limit have surface abundances typical of the less evolved WNL stars, since mass loss is not sufficient to expose more processed matter. This numerical difference explains the shorter duration of the WC phase (and hence correspondingly longer WNL phase) in all our models compared to the results of Meynet (1995). For the same reason the duration of the WNE phase in our models is significantly shorter. Although both the exact behaviour of stars in this mass range and the value of M_{WR} are somewhat uncertain, we feel that the present approach yields a more physical description of the transition between the least massive WR stars and the lower mass stars.

The following important points are illustrated in Figure A2:

- The fraction of Of/O stars (classified by the criterion given in §2.3) is typically of the order of 0.1 to 0.3 for burst ages up to 2-3 Myr. The predicted changes with Z are a result of the differences in the main sequence as a function of Z . Due to the blueward shift of both the zero-age main sequence and the terminal-age main sequence

Table 4: Maximum WR/O ratios

Z	WNL/O			WR/O			
	$\alpha = 1.$	$\alpha = 2.$	$\alpha = 2.35$	$\alpha = 1.$	$\alpha = 2.$	$\alpha = 2.35$	
0.040	1.50	0.54	0.36	1.50	0.54	0.36	($t = 3$ Myr)
0.020	0.51	0.17	0.11	0.97	0.32	0.22	($t \leq 4$ Myr)
0.008	0.23	0.12	0.10	0.40	0.14	0.11	
0.004	0.13	0.058	0.044	0.29	0.091	0.059	
0.001	0.12	0.033	0.020	0.15	0.041	0.025	

(cf. Meynet et al. 1994), the fraction of its main sequence-lifetime a star with an given initial mass spends as an O star increases with lower Z . This leads to the general decrease of Of/O to low Z .

- The *maximum of the WR/O ratio* (and therefore also the WNL/O and WC/O ratios) and the *duration of the WR-rich phase* decrease rapidly with metallicity (cf. Maeder & Meynet, 1994; Meynet 1995). The maximum predicted values are given in Table 4. Note that for $Z < Z_{\odot}$ our WNL/O values are slightly larger than those given by Meynet (1995, his Fig. 6) although both results are based on the same evolutionary tracks. This difference is essentially due to the overestimate by Meynet of the WC population, as discussed above. For $Z \geq 0.020$, the WR/O star number ratio formally becomes infinite at ages $t \geq 4.5$ Myr because the O star population (defined to be those objects with $T_{\text{eff}} \geq 33000$ K) disappears completely while WR stars are still present. Therefore, for these metallicities in Table 4 we give values for the WR/O ratio at specific times $t < 4.5$ Myr (cf. Meynet 1995).
- In an instantaneous burst the WR-rich pe-

riod ($\text{WR/O} > 0$) is characterized by three distinct phases: 1) The **early WNL phase** at the beginning of the WR-rich phase occurs before the most massive stars evolve to WC stars. 2) The **WC-rich or WC-dominated phase** with coexisting WNL stars, where the precise mixture of different WR subtypes depends critically on age and metallicity. 3) The **final WNL phase** with WR stars which have evolved from objects with initial masses close to the lower mass limit of WR formation M_{WR} . Phases occurring before and after the WR-rich period have been discussed by Meynet (1995), to which we refer the reader for more details.

3.1. Frequencies of WR-rich starbursts

An interesting result from the work of Meynet (1995) is the predicted frequency of WR-rich objects in young starbursts. In Table 5 we present the revised frequencies predicted from our models. For an instantaneous burst scenario one can easily determine the time during which the population contains only O stars (“O_{only}”), both WR and O stars (“WR+O”), or WR stars and no O stars (i.e. B instead of O stars: “WR_{only}”). The values given in Table 5 (cols. 2-4) are the fraction of time spent in these phases with respect to the

Table 5: Statistics of H II and WR galaxies. The metallicity is given in col. 1. Cols. 2-6 indicate the predicted fraction of H II regions containing: only O stars (col. 2), WR and O stars (3), WR but no O stars (4). The fraction of H II regions dominated (in number) by WNL stars, and WC stars is given in Cols. 5 and 6. All numbers are relative fractions of the total number of predicted H II regions defined as clusters harbouring O and/or WR stars. Col. 7 indicates the fraction of WR-rich H II regions dominated by WC stars (in number).

Z	O _{only}	WR+O	WR _{only}	WNL	WC	$\frac{\text{WC}}{\text{totalWR}}$
0.040	0.20	0.26	0.54	0.48	0.32	0.40
0.020	0.28	0.36	0.36	0.50	0.22	0.31
0.008	0.40	0.60		0.43	0.17	0.28
0.004	0.60	0.40		0.27	0.13	0.33
0.001	0.82	0.18		0.18		

total time when O and/or WR stars are present. Columns 5 and 6 give the fraction of time during which the WR population is expected to be dominated (in number) by stars of WNL and WC subtypes respectively. The last column (col. 7) gives the fraction of WR-rich starbursts that are expected to be dominated by WC stars (i.e. the values in column 7 are derived by dividing the values in column 6 by the sum of the values in columns 3 and 4). Note that the values in cols. 5-7 differ from those of Meynet (1995, Table 1, high mass loss models) whose results overestimate the relative duration of the WC and WNE phases with respect to the WNL phase as discussed above⁵.

For an instantaneous burst of star formation, the phases during which O and/or WR stars are present in the population should lead to a strong emission line spectrum. Therefore, the fractions given in Table 5 should represent the fraction of H II regions (extragalactic H II regions or alike objects) which should be dominated by the various stellar types. Although comparisons with observations are difficult due to problems regarding the statistical completeness of a given sample, estimates derived from low metallicity samples yield encouraging results regarding both the frequency of the WR phase and the occurrence of WC stars (Schaerer & Vacca 1996). Systematic studies of the WR and O content in statistically complete samples should be possible in the near future.

3.2. WC/WO populations in starbursts

From both observational and theoretical studies it is well known that the subtype distribution of WC stars changes dramatically with metallicity (cf. Smith & Maeder, 1991). In particular, late type WC stars are found only in high metallicity environments (e.g., Conti & Vacca 1991; Philips & Conti 1992), while all WC/WO stars

⁵In Table 1 of Meynet (1995), columns 1 and 2 for the high mass loss models at $Z=0.004$ are misprints. All other values in common with Meynet are in agreement.

are found to be WC4 or WO types in low metallicity regions.

WC stars are expected to evolve towards earlier subtypes during their lifetime, an evolution that reflects the change in surface abundance as larger amounts of processed matter are brought to their surface (Maeder 1991b). Therefore in a burst at a given metallicity, the distribution of WC/WO subtypes is expected to evolve with time. To quantify this behaviour we have calculated the IMF-weighted mean WC subtype (henceforth called IMF-averaged subtype), which reflects the average WC subtype of a mixed population of WC stars. We assigned WO stars to the WC3 subtype. The time evolution of the IMF-averaged WC subtype at different metallicities is plotted in Figure A3. The horizontal lines on the left indicate the average value for regions of constant star formation.

Figure A3 nicely illustrates the qualitative changes of the WC population not only with metallicity but also with time. As expected this figure shows the predominance of WO and early type WC stars at low metallicity. Similarly, at a given Z the average WC subtype decreases with time due to the increase of the surface (C+O)/He abundance ratio along each evolutionary track. Late WC stars are therefore expected only at early times during the WC-rich phase (typically at $t \sim 3\text{--}4$ Myr), or during later times in a high metallicity region.

4. Evolution of the ionizing spectrum

In this Section we discuss the behaviour of quantities directly related to the ionizing flux of the stellar population.

4.1. Ionizing fluxes

Figure A4 presents the predicted time evolution of the photon luminosity in the ionizing continua of hydrogen (Q_0), He I (Q_1), and He II (Q_2). Note that all values are normalised to a population of a total mass of $1 M_\odot$ assuming a

Salpeter IMF from 0.8 to $120 M_\odot$. However, the qualitative properties discussed below are applicable to most IMFs.

The metallicity dependence of the ionizing continuum of an integrated population is determined primarily by variations in the evolutionary tracks; changes due to blanketing effects in the atmosphere models are relatively minor (e.g. Cerviño & Mas-Hesse 1994). The behaviour of the Lyman continuum flux is controlled essentially by the main sequence evolution. In WR-rich phases the maximum contribution to the Lyman continuum provided by these stars is typically $\sim 30\%$ (cf. also below). Main sequence stars also govern the behaviour of Q_1 , although the picture is somewhat more complicated by the fact that WR stars contribute a non-negligible fraction of the He I ionizing flux. In very young bursts (< 3 Myr) the He II ionizing continuum is dominated by O stars. The small differences with metallicity in this case are due to changes in the stellar wind properties, which dominate the opacity in the He II continuum (see Schaerer & de Koter, 1997). During the WR-rich phases Q_2 is clearly dominated by the contribution of WR stars. The time and metallicity dependence of Q_2 is therefore directly related to the duration of this phase and the total number of WR stars present (the “strength” of the WR phase illustrated in Fig. A2).

What implications do the recent stellar atmosphere models have for the predictions of the ionizing flux of a stellar population? As discussed in detail by Schaerer & de Koter (1997) the inclusion of non-LTE effects, line blanketing, and stellar winds in the *CoStar* models leads to significant changes in the ionizing fluxes of O stars. The predictions of these models appear to be supported by observations of H II regions (Stasińska & Schaerer, 1997). Figure A5 illustrates the different predictions for the ionizing fluxes for an instantaneous burst at solar metallicity from the various atmosphere models for O and WR stars. The solid line shows our standard model, using

the *CoStar* models for O stars and the fluxes from Schmutz, Leitherer & Gruenwald (1992) for WR stars. The dashed line was derived using the Kurucz (1992) plane parallel, LTE model atmospheres models instead of the *CoStar* models for O stars. Adopting Kurucz model atmospheres for both O and WR stars (using the wind corrected effective temperature from the evolutionary models) yields the dotted line.

Figure A5 (cf. dotted and dashed) illustrates the importance of using appropriate atmosphere models for WR stars to describe the ionizing fluxes in WR-rich phases (between ~ 3 and 6 Myr). The role of WR stars in this context is discussed in detail by Schmutz, Leitherer & Gruenwald and García-Vargas (1996). As can be seen from Fig. A5 (comparing dashed and solid lines) the inclusion of *CoStar* models for O stars leads to the following changes with respect to synthesis models relying on older (and less complete) stellar atmospheres: 1) In young bursts Q_2 increases by at least 4 orders of magnitudes. The absolute value of the ionizing flux in the He II continuum can therefore reach values similar to those attained during the WR-rich phase. 2) In the first few million years of a burst the He I ionizing flux increases by typically 60 %. 3) Small differences in the Lyman continuum flux are due mostly to larger values of Q_0 for supergiants with $M = 20$ to $40 M_\odot$.

4.1.1. The ionizing flux of WR stars in starbursts

As mentioned above the contribution of WR stars to the ionizing spectrum of a stellar population is not negligible, especially at the shortest wavelengths. In this context, it is interesting to examine the average Lyman continuum luminosity emitted per WR star, $Q_0(\text{WR})/N(\text{WR})$, where $Q_0(\text{WR})$ is the total Lyman luminosity emitted from all WR stars and $N(\text{WR})$ is the number of WR stars present. This quantity is plotted in Fig. A6 where we show the temporal evolution of $Q_0(\text{WR})/N(\text{WR})$ for all metallicities.

ties.

For each metallicity the average Q_0 emitted per WR star generally decreases with time as expected from the decrease of their average luminosity with progressing age. The increase of the maximum average Lyman luminosity (and also of the time-averaged $Q_0(\text{WR})/N(\text{WR})$) with decreasing Z simply reflects the higher average luminosity of WR stars at low Z , or equivalently, the larger value of M_{WR} - the minimum mass of WR formation - at lower Z (cf. § 2.2). It is interesting to note that the average value of Q_0 per WR star shows variations over typically more than one order of magnitude during the WR rich phase. As will be discussed below (§ 8.3) this variation affects estimates of WR/O ratios derived from He II $\lambda 4686$ and $\text{H}\beta$ line strengths; in the past such estimates were calculated assuming a single dominant WR subtype and a constant value of Q_0 per WR star (e.g. $Q_0 = 1.7 \times 10^{49} \text{ s}^{-1}$ for WNL stars, VC92).

5. Evolution of nebular lines of hydrogen and helium

5.1. $\text{H}\beta$

Hydrogen recombination lines, particularly $\text{H}\beta$ serve as a fundamental reference for measurements of other emission lines. In addition, under the assumption of an ionization bounded nebula, their luminosities provide an estimate of the ionizing flux present and their equivalent widths can be used as an accurate indicator of the age of the population in the case of an instantaneous burst of star formation (a coeval population), as first pointed out by Copetti, Pastoriza & Dottori (1986). A critical discussion of this and other age indicators for young starbursts can be found in Stasińska & Leitherer (1996).

The temporal evolution of the $\text{H}\beta$ equivalent width $W(\text{H}\beta)$ for all metallicities is shown in Fig. A7 (left panel). The right panel shows $W(\text{H}\beta)$ only during WR rich phases. The results presented in these figures can be combined with re-

sults presented below (cf. Figs. A14, A15) to determine the WR and O star populations in a region from observational quantities.

5.2. He II $\lambda 4686$

Figure A8 shows the predicted *nebular* He II $\lambda 4686$ emission for all metallicities; this figure was presented in Schaerer (1996c). Here we briefly reiterate the most important points demonstrated in this figure.

For young bursts dominated by O stars ($t \lesssim 3$ Myr) typical values of $I(\text{He II})/I(\text{H}\beta)$ are between 5×10^{-4} and 2×10^{-3} . As mentioned above (cf. § 4), due to the strong He II continuum flux obtained from the most recent and physically complete O star models, these values are ~ 4 order of magnitudes larger than predictions from other current synthesis models. However, the $I(\text{He II})/I(\text{H}\beta)$ values are still too low to be detectable in nebulae around O stars or in young H II regions.

During the subsequent WR rich phase $I(\text{He II})/I(\text{H}\beta)$ values of 10^{-2} to 10^{-1} are obtained. In order to determine which sources contribute to the high value of $I(\text{He II})/I(\text{H}\beta)$ we have plotted the time evolution of $4686/\text{H}\beta$ during the WR phase for two selected metallicities in Fig. A9 (upper left panel: $Z=0.004$, upper right: $Z=0.001$) and the corresponding WR/(WR+O), WNL/(WR+O), and WC/(WR+O) number ratios (lower left panel: $Z=0.004$, lower right: $Z=0.001$). This Figure indicates that large nebular He II/H β values are obtained during the WC/WO phase as well as during a short time before and after the WC phase (cf. Fig. A2 and Schaerer 1996c). The high excitation is provided by WC/WO stars and WN stars that are about to evolve to the former phase. In addition, the relative contributions of WN and WC/WO stars are a strong function of both age and metallicity. This is illustrated by presenting the value of $I(\text{He II})/I(\text{H}\beta)$ obtained when the contribution of WC/WO stars to the ionizing flux is excluded. For $Z=0.004$ almost no change in the line inten-

sity ratio is seen because the nebular He II emission is due primarily to hot WN stars with low hydrogen surface abundances (H mass fraction < 0.1). For $Z=0.001$ the high $I(\text{He II})/I(\text{H}\beta)$ ratio is due mainly to highly evolved WC/WO stars (in this case primarily the WO subtypes, cf. Fig. A3, which have a large Q_2/Q_0) despite their small numbers relative to WN stars. In conclusion, both WC/WO and hot WN stars produce the nebular He II emission. Their relative contributions, however, depend very sensitively on metallicity and (especially) age.

The measurement of the observed flux in a nebular He II $\lambda 4686$ line from a starburst region is complicated by the possible presence of a broad stellar component. In some cases, the narrow nebular component will be superposed on a broad feature (cf. e.g. VC92). However, in many instances, the broad feature may completely dominate the emission, which makes the identification and measurement of a nebular component nearly impossible with low to medium resolution spectroscopy. The interplay between the two components will be discussed in § 6.2.3.

6. Evolution of broad stellar emission lines

In this Section we discuss the behaviour of the broad emission lines included in our calculations (see § 2.2.1). Two different types of illustrations are useful for comparisons with observational data: 1) Plots of the equivalent widths of a feature as a function of age, and 2) Line intensity ratios with respect to H β as a function of the H β equivalent width, which serves as an age indicator. Depending on the spectroscopic observations (type of object, spatial resolution, quality of observations etc.), and several other factors one or the other approach may be favoured. Figures of the first type depend only on stellar quantities, since in most cases nebular continuum emission is fairly small. Equivalent widths may, however, be reduced by an underlying population. Intensity ratios of the WR lines with respect to H β , for example, have the advantage of being rela-

tively independent of such dilution effects. On the other hand comparisons of this type rely on the assumption of an ionization bounded nebula, and may be affected by the relative spatial distribution of the stellar and nebular emission, and the extent of the emission compared to the size of the aperture used for the spectroscopic observations.

6.1. UV lines: He II $\lambda 1640$

Figure A10 shows the temporal evolution of the He II $\lambda 1640$ equivalent width for all metallicities. As with all quantities related to WR stars, the substantial variation with metallicity is due to the strong dependence of WR evolution on Z (cf. Maeder & Meynet 1994). For sub-solar metallicities $W(1640)$ is always predicted to be smaller than $\sim 4 \text{ \AA}$. For these metallicities, the time dependence of $W(1640)$ follows the total WR/(WR+O) ratio quite closely, as discussed in § 8.3.3. Since for $Z > 0.02$ WN stars dominate the 1640 emission (late WC stars have a lower 1640 emission), stronger variations are found between the WC and WN dominated phases.

6.2. Optical lines

6.2.1. *The traditional WR bumps at low spectral resolution*

In Figure A11 we plot the evolution of the equivalent width of the two WR emission blends prominent in the optical wavelength regime; these are the strongest WR features found in the spectra of WR galaxies. Adopting the line fluxes from Tables 1 and 2 we have calculated the 4660 \AA bump (solid line) from the sum of N III/V $\lambda 4640$, C III/IV $\lambda 4650$, and He II $\lambda 4686$; the 5808 \AA emission blend (long-dashed) is due to the C IV multiplet. The 4660 bump may be contaminated by additional nebular emission from He II, He I, and forbidden Fe and Ar lines observation at medium or low resolution, the distinction between the individual components of the bump is often difficult. This makes comparisons to the

total ‘‘bump’’ necessary in many cases, although working with the individual WR lines would be preferred.

As Fig. A11 shows, the equivalent width of the 4660 bump is usually expected to be larger than that of 5808. In WC rich phases, however, $W(5808)$ can reach values comparable to that of 4660. Note that the appearance of the 4660 bump before the WR phase ($0.5 \lesssim t \lesssim 2.5 \text{ Myr}$) is due to stellar He II $\lambda 4686$ emission from OIf stars (cf. below). Compared to the recent models of Cerviño & Mas-Hesse (1994) ⁶our predicted equivalent widths for the 4660 bump are larger by up to a factor of ~ 3 for low Z . The larger values are essentially due to the high mass loss evolutionary tracks adopted in the present work, which lead to larger WR/O star ratios in better agreement with observations (see Maeder & Meynet 1994).

For comparison we also plot the equivalent widths obtained using the bump luminosities of Smith (1991) given in Table 3 (dotted and short-dashed line in Fig. A11). In this case larger EWs for the two WR bumps are expected as can be seen from a comparison of Tables 1 and 2 with 3. Indeed the 4660 bump luminosity from Smith (1991), derived from He II $\lambda 4686$ of 5 LMC WN6-7 stars, represents an upper limit for all LMC WN stars (cf. Vacca 1992), even if the N III/V $\lambda 4640$ contribution is included. It must, however, also be reminded that N III/V $\lambda 4640$ seems to be metallicity dependent (cf. § 2.2.1). We feel that, for most cases, our procedure of allowing for the strong variations of WC subtypes and including more recent calibrations for WN stars should yield more reliable predictions for the WR bumps than calculations based on the data of Smith (1991).

Figure A12 shows the relative WRbump/H β line intensities of the two bumps. Given the

⁶Their adopted WR bump luminosities are $L_{4660} = 2 \times 10^{36} \text{ erg s}^{-1}$ for WN stars and $L_{4650} = 6 \times 10^{36} \text{ erg s}^{-1}$ for WCs, which differ by $\sim 20\text{-}15\%$ from our values for WNL and WC4 stars.

steepness of the spectrum the maximum intensity ratio $5808/H\beta$ is considerably smaller than $4660/H\beta$ in contrast to the maximum of the equivalent widths (cf. above). The strong increase of the peak $4660/H\beta$ with metallicity is in large part due to the much more rapid decrease of $H\beta$ for large metallicities (cf. Arnault, Kunth & Schild 1989).

6.2.2. *WR bumps at medium and high spectral resolution*

In Figure A13 we plot the time evolution of the equivalent widths of all individual WR lines (except $H\alpha$ and $H\beta$; cf. § 6.2.4). The inclusion of 4686 \AA emission from Of stars, although its strength is considerably uncertain, leads to typical values of $W(4686) \sim 1\text{-}2 \text{ \AA}$ before the appearance of the first WR stars ($t \lesssim 2\text{-}3 \text{ Myr}$). During the WN dominated phases the strongest lines are He II $\lambda 4686$, N III/v $\lambda 4640$ and C IV $\lambda 5808$ in decreasing order. The weakness of N III/v $\lambda 4640$ at subsolar metallicity is due to the metallicity-dependence of this line (SSM96). For solar and higher metallicities N III/v $\lambda 4640$ is expected to have a strength comparable to He II $\lambda 4686$ (Smith 1991, SMM96). In the WC-rich phase C III/IV $\lambda 4650$ is expected to dominate the 4660 bump ($W(4650)/(W(4640)+W(4686)) > 1$). Interestingly, for a given metallicity at $Z > 0.001$, the maximum equivalent width attained for the 4650 bump, He II $\lambda 4686$ and C IV $\lambda 5808$ are all of the same order. Since late WC stars are only expected at high metallicities (cf. § 3.2) the maximum equivalent width of C III $\lambda 5696$ only reaches values above $\sim 1 \text{ \AA}$ for $Z \geq 0.02$. At subsolar metallicities the equivalent width of He II $\lambda 5412$ is found to follow closely that of N III/v $\lambda 4640$. In all cases $W(5412)$ is less than 2 \AA .

Figures A14 (for $Z=0.008, 0.004,$ and 0.001) and A15 (for $Z=0.02$ and 0.04) show the ratios of the WR lines with respect to $H\beta$ as a function of the $H\beta$ equivalent width. These Figures involve purely observational quantities and can be used for direct comparisons with integrated

spectra of a young burst population (with the aforementioned cautions in mind). Note that for all metallicities He II $\lambda 4686/H\beta$ represents the maximum $WR/H\beta$ intensity ratio obtained in a burst, although the maximum 4650 and 5808 equivalent widths are comparable or even larger than $W(4686)$. This is essentially due to stronger $H\beta$ emission during the WC-rich phase at earlier ages, while 4686 emission from WN stars persists until later times where $H\beta$ has already considerably decreased.

6.2.3. *Nebular and stellar He II $\lambda 4686$*

The case of He II $\lambda 4686$ deserves closer examination. As discussed in § 5 the models predict a non-negligible nebular He II $\lambda 4686$ emission during part of the WR-rich phase. It is therefore expected that the 4686 \AA feature consists of both broad stellar and narrow nebular emission. Although observationally the distinction between narrow and broad components is not necessarily straightforward and has not generally been made, it is crucial for our understanding of excitation conditions and WR populations especially in low metallicity objects (cf. Garnett et al. 1991, and references therein; Schaerer 1996c, Izotov et al. 1996). A detailed discussion of the origin of nebular He II and comparisons with recent observations will be presented elsewhere. Here we shall present only the main theoretical predictions.

Figure A16 shows the intensity ratios $\lambda/H\beta$ of pure nebular He II $\lambda 4686$ (lower left) and both nebular and total WR+nebular 4686 emission (upper left) for metallicities $1/20 \leq Z/Z_{\odot} \leq 1/5$ as a function of $W(H\beta)$. For lower $H\beta$ equivalent widths (i.e. larger ages) 4686 is always dominated by stellar emission, and is therefore not shown here. The same also holds for solar and higher metallicities, as discussed by Schaerer (1996c). In the early phase of the burst nebular He II $4686/H\beta$ reaches values up to $\sim 1\%$, the maximum value being nearly independent of metallicity. Since nebular 4686 emission is related to

WC/WO stars and their hot WN star precursors (cf. § 5) whose population diminishes with Z , the duration of the phase with strong nebular emission is also predicted to decrease. At $Z = 0.001$, the current models predict that He II $\lambda 4686$ is dominated by stellar emission.

In Fig. A16 we have also plotted the predicted C III/IV $\lambda 4650$ emission which is due to WC/WO stars. As mentioned earlier (§ 2.2.1) this blend includes C III $\lambda 4650$, C IV $\lambda\lambda 4650, 4658$ and a small fraction of He II $\lambda 4686$. Interestingly, at $Z = 0.008$ and 0.004 , the predicted 4650 emission has a strength similar to that of the total 4686 emission. It should be remembered, however, that at low Z , WC4 or WO stars are the dominant WC subtypes (Fig. A3). In view of the strong variation of the adopted C IV emission lines between WC4 and WO stars (see Table 2) and present uncertainties in the assignment of WC/WO subtypes (cf. Smith & Maeder 1991, Kingsburgh, Barlow & Storey 1995), the predictions for 4650 remain somewhat uncertain.

If nebular He II emission is indeed related to the WC/WO phase, one expects to detect other signatures for these stars. A nearly unambiguous signature from WC/WO stars is C IV $\lambda 5808$ whose strength is shown in Fig. A15. However, the same word of caution regarding the strength of 4650 also applies to the strength of 5808. The detection of O IV $\lambda 3400$, O VI $\lambda 3811, 34$, or O V $\lambda 5590$ would be a clear signature of WO stars (see Kingsburgh, Barlow & Storey 1995). Test calculations with the current models, however, predict very small equivalent widths for these features.

6.2.4. Broad H α and H β components

The predicted emission in the He II $\lambda 4861 + \text{H}\beta$ blend (denoted as 4861 in Tables 1 and 2) and in the He II $\lambda 6562 + \text{H}\alpha$ blend (denoted as 6560) is illustrated in Fig. A18 for all metallicities. For subsolar metallicities equivalent widths of $\sim 5\text{-}25$ Å for 6560 and $1\text{-}3$ Å for 4861 are predicted. For solar and larger metallicities stronger emission is expected.

The line strengths predicted in this work do not include stellar absorption features. Such predictions for young bursts have been given by Olofsson (1995a) who synthesized the major H and He absorption lines for instantaneous bursts at metallicities $Z \leq Z_{\odot}$. For the ages shown in Fig. A18 his predicted equivalent widths (absorption) are: $2\text{-}4$ Å for H α and $2\text{-}5$ Å for H β for the range of IMF considered. The strength of the absorption lines is fairly independent of metallicity (Olofsson 1995a). (Note, however, that for unknown reasons the EWs of the Balmer lines predicted by Olofsson are systematically smaller than those of Díaz 1988.) The comparison with the results of Olofsson (1995a) shows that during the WR phase the equivalent width of the H α emission from WR stars is larger than the equivalent width of the underlying absorption. The net result of the superposition depends, of course, on the relative widths of the two components.

The strength of the stellar 6560 Å emission is compared to that of the nebular emission in Figure A18. For low metallicities the WR emission may reach several percent of the nebular flux, whereas much larger contributions are expected at solar and higher metallicity. This effect is bolstered by both the increase of the WR population and the lower ionizing flux. As can be seen from Table 1 and 2 the relative 6560/4861 line emission in WR stars varies between 1.6 and 6. For an integrated population a typical value of this ratio is found to be $\sim 4\text{-}5$, which is larger than the value of H α /H β =2.86 for Case B recombination. Thus, the relative contributions of WR emission to the nebular H α and H β lines may, in principle, affect reddening determinations derived from these lines. However, the uncertainties on the WR line emission in these lines are fairly large (cf. Tables 1, 2).

Obviously the broad H α and H β emission components discussed here occur only during the WR phase, which is best detected by the presence of WR bumps that are uncontaminated (or only weakly contaminated) by nebular emission. In

this case the flux in the broad 4861 Å emission provided by WNL stars is typically $\sim 25\%$ of the flux in the total 4650 bump, while it is negligible for WC stars (cf. Tables 1, 2). Additional broad emission which may be present (e.g. Roy et al. 1992, Izotov et al. 1996) cannot be attributed directly to WR stars.

7. Models including massive close binary stars

The main results derived from models in which binary stars are included according to the prescriptions in §2 are illustrated in Figures A19 and A20, for metallicities $Z=0.008$ and 0.001 . (The results for the remaining metallicities show the same qualitative behaviour and therefore are not reproduced here.) The top panel shows the relative fraction of WR stars of different subtypes. The use of WR/O number ratios (as e.g. shown in Fig. A2) is avoided for two reasons. First, in the phase where the WR stars are formed through the binary channel ($t \gtrsim 5$ Myr) the number of single O stars is usually either low or possibly zero. Second, in order to compute such ratios one also needs to account for O stars formed from the mass-gainer in the binary systems (whose fate is not followed in the current calculations). In any case, as discussed earlier, it is advisable to directly use diagrams involving only observable quantities (cf. bottom panel). The middle panel shows the time evolution of the equivalent widths of the strongest WR lines (He II $\lambda 4686$ and C IV $\lambda 5808$) as a function of time. The intensities of the same lines with respect to $H\beta$ are plotted in the bottom panel as a function of the $H\beta$ equivalent width.

Accounting for the WR formation in massive close binary systems obviously extends the period where WR stars are present in instantaneous bursts (see top panels), since their progenitors can have masses smaller than the WR mass limit for single stars. For the binary models adopted here, WR stars can be present up to ages of $\sim 11-13$ Myr. However, this period can be even

longer (ages up to $\sim 15-20$ Myr) if the possible evolution of the secondary to the WR phase is also included in the model (Cerviño, Mas-Hesse & Kunth 1996, Vanbeveren, Van Bever & Donder 1997). In sharp contrast to burst models which include only single stars, the total duration of the WR phase is now essentially independent of metallicity.

The time evolution of the relative fraction of the different WR subtypes (top panels) is easily understood by combining the results given in Fig. A2 and Fig. 3 from de Loore & Vanbeveren (1994), which give lifetimes in the WNL, WNE and WC phases as a function of the initial primary mass. The formation of WR stars through the binary channel extends the final WNL phase of single stars (cf. §3) to later ages, leads to a second WC-rich period, and results in a significant phase dominated by WNE stars after about 7-8 Myr. However, the following caveat regarding the WR subtype distribution in close binary systems should be kept in mind: As shown by Vanbeveren (1995) the predicted WC/WN number ratio for low metallicity regions with constant star formation exceeds the observed values. One possible explanation is that the duration of the WC phase predicted from binary models is too long. Indeed the different observed WR fractions are well reproduced if RLOF leads to WR stars of mostly WNE type (see Maeder & Meynet 1994). Therefore, the relative distribution of WC and WNE subtypes in the binary phase should be considered fairly uncertain.

The temporal evolution of the predicted equivalent widths of 4686 and 5808 (see middle panel) shows two main characteristics: 1) The phases where WR stars are formed predominantly through the single and the binary channels are well separated. This behaviour, which is obviously true only for short bursts, is a direct consequence of the different progenitor masses from single and binary stars. 2) The expected maximum equivalent width of He II $\lambda 4686$ (C IV $\lambda 5808$) during the binary dominated phase is $\sim 0.5-2$ (2-4)

Å, and is fairly independent of Z . 3) At low Z ($Z \lesssim 0.001$) the maximum equivalent widths of the WR features during the “binary dominated” phase become comparable or even stronger than those during the preceding “single star” phase.

The bottom panel of Figs. A19 and A20 shows the predicted line ratios of $4686/H\beta$ and $5808/H\beta$ as a function of the $H\beta$ equivalent width. As above the two phases where WR originate mostly from pure stellar wind mass loss (“single star channel”) or from RLOF (“binary channel”) are well separated. For $Z \geq 0.004$ ($Z=0.001$) the binary-dominated phase corresponds to $W(H\beta) \lesssim 40$ (100) Å. The $H\beta$ equivalent width (or other age indicator) should thus roughly provide a means to identify burst regions where WR formation through RLOF may be of importance (see also Schaerer & Vacca 1996). Due to the strongly decreasing $H\beta$ luminosity the WR/ $H\beta$ line ratios during the late binary phase can easily exceed the values during the early single-star dominated phase. The maximum line ratios of $4686/H\beta$ and $5808/H\beta$ obtained for the lowest metallicities are typically 5 to 10 % of $H\beta$ for the adopted binary fraction. These values might be overestimated by a factor of ~ 2 if at low Z the binary frequency is actually lower than the adopted value (cf. §2.1.2).

Regarding the predictions including massive close binary systems we wish to stress again the numerous uncertainties mentioned in §2.1.2. It is certainly true that our current knowledge of the evolution of binary stars is less accurate than that of single stars. In addition, in view of the simplified treatment adopted here for binary systems we regard the detailed predictions as explorative and warn the reader from an overinterpretation of this data. The general conclusions should, however, be fairly reliable.

8. On determining the WR and O star content in H II regions and starbursts

The absolute number of WR and O stars, as well as the relative WR/O star number ratios in starburst regions, have been estimated with various techniques (e.g. Kunth & Sargent, 1981; Arnault, Kunth & Schild 1986; Leitherer, 1990; Mas-Hesse & Kunth 1991a, VC92, Vacca 1994; Cerviño & Mas-Hesse 1994; Meynet 1995; Schaerer 1996c). Knowledge of the absolute numbers of stars constituting a population can be used to determine quantities such as the star formation efficiency or rate in a region; relative WR/O star number ratios can be used in conjunction with stellar evolution models to constrain parameters such as the burst duration and the IMF slope, and to understand the variation in population parameters with metallicity.

Rough estimates of the WR and O star content in a starburst region can be obtained in a straightforward way. However, as demonstrated by Schaerer (1996c), more accurate techniques are required to obtain reliable constraints on both the O star content (cf. Vacca 1994) and the IMF (cf. Meynet 1995; Contini, Davoust & Considère 1995). In the following we will therefore review the various methods employed and discuss procedures that should yield the most accurate results.

8.1. Determination of the number of O stars

Usually the number of O stars present in an integrated population is estimated from comparing 1) the total UV continuum luminosity with the predictions of evolutionary synthesis models (e.g. Leitherer & Heckman 1995), or 2) the observed strength of the H recombination lines with predictions of the ionizing fluxes from stellar atmosphere models (e.g. Osterbrock 1989). Here we shall concentrate on the latter procedure, which has been discussed extensively by Vacca (1994, and references therein).

8.1.1. Using H recombination lines

This method is based on the premise that the number of ZAMS O V stars can be directly related to the observed H β luminosity (cf. Vacca 1994). The ionizing flux (in terms of the total number of H-ionizing photons, Q_0^{Total}) required to produce the H β line luminosity $L(\text{H}\beta)$ is given by

$$Q_0^{\text{Total}} = \frac{\alpha_B(\text{H}^0)\lambda_{\text{H}\beta}}{\alpha_{\text{H}\beta}^{\text{eff}}hc} L(\text{H}\beta) \quad (7)$$

(cf. Eq. 4 with $f_\gamma = 1$). Note that Eq. 7 assumes a dust-free and ionization-bounded H II region (Case B recombination). If the stellar population is the only source of ionizing photons, Q_0^{Total} can be expressed in terms of the number of so-called “equivalent” stars of a given subtype (here we use N'_{O7V} to denote the number of “equivalent O7V” stars) responsible for producing the ionizing luminosity,

$$Q_0^{\text{Total}} = N'_{\text{O7V}} Q_0^{\text{O7V}}, \quad (8)$$

where Q_0^{O7V} is the Lyman continuum luminosity of an individual O7V star. As shown by Vacca (1994) the number of ZAMS O V stars is then related to N'_{O7V} by

$$\eta_0 \equiv N'_{\text{O7V}}/N_{\text{OV}}, \quad (9)$$

where

$$\eta_0 = \frac{\int_{M_{\text{low}}}^{M_{\text{up}}} \Phi(M) Q_0^{\text{ZAMS}}(M) dM}{Q_0^{\text{O7V}} \int_{M_{\text{OV}}}^{M_{\text{up}}} \Phi(M) dM}, \quad (10)$$

represents the IMF averaged ionizing Lyman continuum luminosity of a ZAMS population normalized to the output of one “equivalent” O7V star (see Vacca 1994). In Eq. 10, Φ represents the IMF with the mass limits M_{low} and M_{up} , and $Q_0^{\text{ZAMS}}(M)$ is the Lyman continuum luminosity as a function of stellar mass for ZAMS stars. The number of ZAMS O V stars is thus given by

$$N_{\text{OV}} = \frac{Q_0^{\text{Total}}}{\eta_0 Q_0^{\text{O7V}}}. \quad (11)$$

The number of ZAMS O V stars can thus be easily derived from the observed H β luminosity using the extensive tables of Vacca (1994) which provide η_0 for different assumptions of the IMF slope, mass limits and metallicity. For a Salpeter IMF and an upper mass cut-off of $120 M_\odot$ e.g., η_0 is found to be close to unity.

However, for comparisons with evolutionary models and other applications it is crucial to distinguish further between ZAMS O V stars and O stars in general. Indeed, for instantaneous bursts the number of ZAMS O V stars obtained from the above procedure approximates the total number of O stars (of all luminosity classes) only for ages less than $\sim 2\text{-}3$ Myr, as demonstrated by Schaerer (1996c). For larger ages, N_{OV} derived with the method of Vacca (1994) generally *overestimates* the true number of O stars, if one does not appropriately reduce the upper mass limit. Nevertheless, the procedure of Vacca (1994) can be easily generalized to account for the temporal evolution of the total ionizing luminosity and thus to derive the total numbers of O stars. Accordingly, Schaerer (1996c) introduced the time dependent value of η_0 :

$$\eta_0(t) = \frac{\int_{M_{\text{low}}}^{M_{\text{up}}} \Phi(M) Q_0(M, t) dM}{Q_0^{\text{O7V}} \int_{M_{\text{O}}}^{M_{\text{up}}} \Phi(M) dM}, \quad (12)$$

where $Q_0(M, t)$ is the ionizing luminosity of a star of initial mass M at time t . Note that for the integral in the denominator, the identical definition for O stars is used as in the evolutionary synthesis models. With Eq. 12 the total number of O stars is now given by

$$N_{\text{O}} = \frac{Q_0^{\text{Total}}}{\eta_0(t) Q_0^{\text{O7V}}}. \quad (13)$$

The temporal evolution of $\eta_0(t)$ for our “standard” instantaneous burst models is shown in Fig. A21 for all metallicities considered in this work. As expected, the ZAMS values ($\eta_0(t=0)$) agree well with the results of Vacca (1994) using the same IMF. Fig. A21 shows that η_0 remains

fairly constant within the first ~ 2 Myr, and then decreases due to the evolution of the O star population and the subsequent disappearance of the most massive stars (cf. Schaerer 1996c). For subsolar metallicities a short-lived peak of η_0 is found at the beginning of the brief WR-rich phase ($t \sim 3$ Myr) due to the large average Lyman continuum luminosity of WR stars at this time (cf. Fig. A6). The second, brief increase in η_0 seen in several of the panels occurs when the number of O stars (as defined by the lower limit on T_{eff}) drops to zero, and hence the denominator in Eq. 12 approaches zero. Obviously, the definition of η_0 becomes meaningless at this time; the ionizing flux of the population will be provided by stars of B type or later and WR stars which may still be present in some cases ($Z \geq 0.02$).

Although more general than the formulation of Vacca (1994), the explicit time dependence of $\eta_0(t)$ introduces two new variables that must be determined before this quantity can be used to determine the massive star population in a region. In addition to the assumptions about the IMF (slope and mainly upper mass limit) and metallicity, the value of $\eta_0(t)$ also depends on the age of the stellar population and the star formation history, for which we have only considered the case of an instantaneous burst here. In most cases, the observed $H\beta$ equivalent width can be used to estimate the population age (see Fig. A7). The star formation history is somewhat more problematic, as this is usually one of the parameters trying to be determined. Note that the procedures and limitations discussed here also apply in principle to methods which estimate the O star content from the UV continuum luminosity. However, these methods tend to be less sensitive to variations in the population parameters and avoid other potential difficulties affecting the nebular lines (photon leakage etc.).

8.1.2. Using He recombination lines

An equivalent of the above procedure can be formulated using the He I $\lambda 4471$ line, which relies

on Q_1 the total He I ionizing luminosity emitted by the stellar population (cf. Vacca 1994). However, since stars with $T_{\text{eff}} \gtrsim 40000$ K provide enough photons above 24.6 eV to fully ionize helium, the ratio of the ionic fractions of He I and H I in the nebula becomes independent of T_{eff} (see e.g., Doherty et al. 1995). In this case He I does not provide any additional information compared to H recombination lines. In particular He I $\lambda 4471/H\beta$ will be insensitive to variations in the IMF (both slope and upper mass limit) as long as enough hot stars are present in the population to keep the “equivalent” effective temperature above ~ 40000 K.

The situation is even more complicated for other He I lines, e.g. the He I $\lambda 2.06 \mu\text{m}$ line, whose predicted strength is dependent on assumptions about the structure of the H II region (cf. Shields 1993). Lines resulting from recombination of He^{++} are rarely detected in H II regions and their origin is not fully understood (cf. Schaerer 1996c and references therein). During the pure O star phase of a burst (cf. § 3) the He II $\lambda 4686/H\beta$ is most likely too weak to be detected. In later phases WR stars (or other poorly understood processes) dominate the formation of nebular He II lines. See § 5 for more details.

8.2. Determination of the number of WR stars

The total number of WR stars, and their relative subtype distribution, can be easily determined from the observed luminosity in a given broad WR line in the integrated spectrum of a starburst region (e.g., Osterbrock & Cohen 1982; Kunth & Sargent 1983; VC92). The reliability of this method obviously rests on the constancy of the line luminosity for all WR stars (cf. § 2.2.1) and a correct measurement of the desired WR component of the line, which is often a composite of different WR lines (see § 2.2.1) or blended with nebular emission (e.g. [Fe III] $\lambda 4658$, [Ar IV] $\lambda\lambda 4711, 4740$).

8.3. Determination of WR/O number ratios

Two different methods have been developed to derive WR/O star number ratios from optical spectra of integrated populations. While the method of Arnault, Kunth & Schild (1986) uses the flux in the entire WR bump, the more recent work of VC92 relies only on the flux in the broad He II $\lambda 4686$ line. In the following we will briefly discuss and compare these two methods, point out their respective advantages, and present some improvements on these techniques.

8.3.1. From He II $\lambda 4686$ and H β

Following VC92, we can write the ratio of the number of WR stars to the number of reference O7V stars as

$$\frac{N_{\text{WR}}}{N'_{\text{O7V}}} = \left(\frac{Q_0^{\text{O7V}}}{Q_0^{\text{WR}}} \right) \left[\left(\frac{Q_0^{\text{Total}}}{N_{\text{WR}} Q_0^{\text{WR}}} \right) - 1 \right]^{-1} \quad (14)$$

where Q_0^{WR} is the average Lyman continuum luminosity per WR star. The total number of WR stars is given by the luminosity of the broad WR line,

$$N_{\text{WR}} = L_{\text{obs}}(\lambda_{\text{WR}})/L_{\text{WR}}(\lambda_{\text{WR}}), \quad (15)$$

where λ_{WR} represents one particular WR line (e.g. He II $\lambda 4686$), and $L_{\text{WR}}(\lambda_{\text{WR}})$ is the line luminosity for a single WR (e.g. WN) star. Inserting Eqs. 7, 12, and 15 in Eq. 14 one finds,

$$\frac{N_{\text{WR}}}{N_{\text{O}}} = \eta_0(t) \left[\left(\frac{\alpha_B(\text{H}^0)\lambda_{\text{H}\beta}}{\alpha_{\text{H}\beta}^{\text{eff}}hc} \right) \frac{L_{\text{WR}}(\lambda_{\text{WR}})}{Q_0^{\text{O7V}}} \frac{L_{\text{obs}}(\text{H}\beta)}{L_{\text{obs}}(\lambda_{\text{WR}})} - \frac{Q_0^{\text{WR}}}{Q_0^{\text{O7V}}} \right]^{-1} \quad (16)$$

For the nebular conditions assumed here (cf. § 2.3) $\alpha_B(\text{H}^0)\lambda_{\text{H}\beta}/(\alpha_{\text{H}\beta}^{\text{eff}}hc) = 2.1 \times 10^{12} \text{ erg}^{-1}$. In addition to the assumptions stated earlier regarding the presence of dust and leakage of ionizing photons (cf. § 8.1), Equation 16 assumes that the ionization is provided completely by the population of N_{O} O stars and N_{WR} WR stars

with a Lyman continuum luminosity Q_0^{O} and Q_0^{WR} , respectively. Furthermore it is assumed that only stars of the generic subtype ‘‘WR’’ contribute to the WR line in consideration. Vacca & Conti (1992) considered the case where only WNL stars are present. They adopted the values of $L_{\text{WNL}}(\lambda 4686) = 1.7 \times 10^{36} \text{ erg s}^{-1}$, $Q_0^{\text{WNL}} = 1.70 \times 10^{49} \text{ s}^{-1}$, and $Q_0^{\text{O7V}} = 1.01 \times 10^{49} \text{ s}^{-1}$, in Eq. 15 of VC92 for $\eta_0(t) = 1$.

We will now try to estimate the accuracy of the procedure of VC92, or more generally of Eq. 16. In addition to the age of the population and the star formation history (needed for η_0 ; § 8.1), use of Eq. 16 requires an estimate of $Q_0^{\text{WR}}/Q_0^{\text{O7V}}$, the ratio of the average Lyman continuum luminosity emitted per WR star to the Lyman continuum output of the equivalent O7V star. As shown in Fig. A6 large variations of Q_0^{WR} are expected during the evolution of a burst. Values of $\log Q_0^{\text{WR}} > 49.05$ (i.e. $Q_0^{\text{WR}}/Q_0^{\text{O7V}} > 1.68$) yield larger WR/O ratios than those derived using Eq. 15 of VC92. However, for the typical values of He II $\lambda 4686/\text{H}\beta < 0.1$ observed in starburst regions, an average value of Q_0^{WR} below the value used by VC92 yields negligible changes in $N_{\text{WR}}/N_{\text{O}}$.

Equation 16 accounts for the presence of one dominant WR subtype, e.g. WNL stars as assumed by VC92. However, as discussed in § 3, variations in the subtype distribution are expected as a burst population ages. Although an appropriate WR line, whose flux is due primarily to WR stars of a certain subtype (i.e. 4686 Å by WNL stars, or 5808 Å by WC stars) could easily be chosen in the case of a mixed population, for Eq. 16 to be valid the representative WR subtype must also contribute the bulk of the ionizing flux from the total WR population.

In conclusion we stress again (cf. Schaerer 1996c) that variations of $\eta_0(t)$ and Q_0^{WR} complicate the derivation of accurate WR/O number ratios from He II $\lambda 4686/\text{H}\beta$ using the method devised by VC92. For detailed comparisons with evolutionary models and reliable estimates of

other parameters like the IMF slope etc., it is preferable to use models such as those developed in the present work, which allow a direct comparison of all relevant observational quantities (see Sects. 6) and thereby circumvent the difficulties discussed above.

8.3.2. From the “WR-bump” and $H\beta$

From the first synthesis models of WR and O star populations Arnault, Kunth & Schild (1986) proposed an approximate fit relation to derive an estimate of the total WR/O ratio (for all WR subtypes) from the ratio of the WR bump luminosity to $H\beta$. To the level of accuracy considered in their work the results for a given IMF slope were found to be fairly insensitive to the star formation scenario and metallicity. Despite this insensitivity, to the best of our knowledge the fit relation proposed by Arnault, Kunth & Schild (1986) has not been used in the literature to estimate WR/O ratios. With the new models presented in this work, which rely on more complete input physics, we have reexamined the results of Arnault, Kunth & Schild (1986). To calculate the total emission in the WR bump, we sum the individual contributions of N III/IV $\lambda 4640$, C III/IV $\lambda 4650$ and He II $\lambda 4686$ from WN and WC stars. Figure A22 shows the WR/(WR+O) ratio as a function of the predicted WR-bump/ $H\beta$ ratio for all instantaneous burst models (thin lines).

As anticipated from the results of Arnault, Kunth & Schild, the data show reasonably well-defined relation extending over at least 2 orders of magnitude in WR-bump/ $H\beta$. Our data can be fitted by

$$\log \left[\frac{\text{WR}}{\text{WR} + \text{O}} \right] = (-0.11 \pm 0.02) + (0.85 \pm 0.02) \log \left(\frac{\text{WR}_{\text{bump}}}{H\beta} \right) \quad (17)$$

(thick solid line labeled SV) with a rms of 0.22 dex. As discussed below (cf. § 6.2.1), the detailed predictions show notable differences if we adopt the WR bump luminosities of Smith (1991,

cf. Table 3). The average fit relation is, however, only slightly changed by this assumption. For comparisons the thick dotted line (labeled AKS86) shows the fit relation from Arnault, Kunth & Schild (1986). Although our detailed predictions reveal large differences with the results of Arnault, Kunth & Schild (1986), the derived fit relations agree relatively well.

We have also compared the model predictions with the WR/(WR+O) ratio derived from Eq. 16 assuming $\eta_0(t) = 1$, $Q_0^{\text{WR}}/Q_0^{\text{O7V}} = 1.68$ and two values of the WR-bump luminosity $L_{\text{WR}}(\lambda\text{WR}) = 1.7 \times 10^{36} \text{ erg s}^{-1}$ (thick long-dashed line) and $5. \times 10^{36} \text{ erg s}^{-1}$ (thick short-dashed line) respectively. The long-dashed line thus corresponds to Eq. 15 of VC92, while the short-dashed line stands for the upper limit of the WR-bump luminosity (WC stars from Smith 1991). The comparison of both curves with the model predictions confirm the finding that in general the method of VC92 *overestimates* the WR/O ratio. The largest differences are obtained for large values of WR-bump/ $H\beta$, which are expected at late epochs in bursts. In this case the difference is due to the assumption of an unevolved ZAMS population, i.e. $\eta_0 = \text{const}$ (cf. above).

We conclude that Eq. 17 is useful for estimates of the total WR/(WR+O) ratio from relatively low resolution integrated spectra of starburst regions. As a word of caution it must be mentioned that such a relation does *not* hold for the He II $\lambda 4686/H\beta$ (or even for C IV $\lambda 5808/H\beta$) as can be seen from Figs. A2 and A14. The fit relation also requires that all possible contamination from nebular lines (cf. § 8.2) to the WR bump be excluded before it can be used to determine the WR/O star number ratio. In general it may not be possible to do this.

8.3.3. From UV spectra

Since the luminosity of WN and early WC stars in the He II $\lambda 1640$ line is quite similar (see Tables 1 2), and since O stars are the dominant contributors to the UV continuum, the equiva-

lent width of He II $\lambda 1640$ is expected to be closely related to the ratio of the total number of WR stars to O stars. Indeed, as Fig. A23 shows, our models predict a relatively well-defined relation between $W(1640)$ and $WR/(WR+O)$, which can be fitted by

$$\log \left[\frac{WR}{(WR+O)} \right] = (-1.31 \pm 0.03) + (1.52 \pm 0.05) \log (EW(1640)) \quad (18)$$

with a rms of 0.29 dex (thick solid line in Fig. A23), where $W(1640)$ denotes the equivalent width of the broad stellar He II $\lambda 1640$ emission in \AA . Note that in this fit we have excluded the points with $WR/(WR+O)=1$, corresponding to bursts with ages $t \gtrsim 3\text{-}4$ Myr at $Z \geq 0.02$.

Equation 18 can be used to obtain estimates of the total WR/O ratio from a pure equivalent width measurement in cases where the rest-frame UV is the only accessible wavelength range (e.g. high redshift galaxies), or if the optical spectrum is strongly contaminated by old populations. As long as there is no emission component from an active galactic nucleus, the He II $\lambda 1640$ line also has the advantage of being independent of nebular lines, which may be subject to additional complications, as mentioned above. For more precise determination of the WR and O star content, comparisons with the detailed model predictions discussed in § 6 should be preferred over the use of Eq. 18.

9. Summary

We have constructed new evolutionary synthesis models for young starbursts using the latest stellar evolution tracks, theoretical spectra generated with the most complete input physics, and a compilation of observed emission line strengths for WR stars. To provide predictions for various stellar and nebular emission line strengths, our models account explicitly for the contributions of WR stars of different subtypes. We have also explored the consequences of WR formation through mass transfer in close binary systems.

9.1. Predicted observational features

The models presented here, and their predictions for various emission line strengths, can be used to derive massive star populations in starburst regions. Comparisons between observed and predicted line strengths allow the derivation of several properties characteristic of a starburst (e.g. burst age and duration, IMF, mass). In particular, we synthesize seven different WR emission lines, including one UV line. We also predict the strength of the various nebular and stellar components contributing to the so-called WR-bump ($\lambda \sim 4650 \text{\AA}$). These lines, whose emission strengths vary considerably among the various WR subtypes, provide a means of deriving the numbers of both WN and WC stars in a starburst region. The model predictions for the nebular lines provide a measure of the O star population. In addition, our models provide the first quantitative predictions regarding a possible origin for nebular He II emission which is frequently observed in low metallicity H II regions (e.g. Garnett et al. 1991). We also estimate the contribution of WR emission to broad components seen underlying $H\alpha$ and $H\beta$ lines in the spectra of H II regions (e.g. Roy et al. 1992). Taken together these diagnostic features should allow the most accurate determination of massive star populations in young bursts to date.

9.2. Stellar evolution in different environments and tests of the models

Models of massive star evolution and atmospheres have not been extensively tested in regions outside of the solar vicinity. It is particularly important to understand the role metallicity plays in determining the characteristics of massive stellar atmospheres and evolution. Our models can be used to study the evolution of massive stars in environments which are not accessible “locally” (e.g. in very low or very high metallicity regions), and therefore they can be used to test the models of stellar evolution and stel-

lar atmospheres under diverse and extreme conditions. For example, by comparing our model predictions with the parameters derived from integrated spectra of starforming clusters whose stellar content and burst properties can be determined by other means, the effects of metallicity and environment on massive star properties and populations can be probed. Although such studies have only recently begun for LMC and SMC clusters whose content is known from stellar censuses (i.e., from imaging and direct counting; Vacca et al. 1995; Vacca & Conti 1997), they will serve as touchstones for evolutionary synthesis models. Similar studies can be carried out for other star-forming regions where individual stars can be resolved with HST. It is particularly interesting to extend such studies to extremely metal poor galaxies (e.g., I Zw 18, Hunter & Thronson 1995).

There are several observational studies that can be carried out to test the validity of our models: 1) Determination of the frequency of WR rich starbursts and the frequency of WC detections among WR galaxies, as first suggested by Meynet (1995) (see §3). 2) Examination of the predicted relation between nebular He II $\lambda 4686$ and a population of WC/WO and/or hot WN stars (cf. §5). 3) Searches for WR signatures in old bursts, which may be indicative of WR stars formed through mass transfer in close binary systems (§7). The first investigations along these lines have recently begun (Schaerer 1996c, Schaerer et al. 1997).

Of particular interest in this regard is the analysis of the optical spectra of the recent samples of low metallicity extragalactic H II regions, used for the determination of the primordial He abundance (e.g. Izotov, Thuan & Lipovetsky 1997; Olive, Skillman & Steigman 1997). These objects are ideal for testing the evolutionary and atmospheric models in low Z environments. This is nicely illustrated by the recent detection of WC stars in I Zw 18 (Izotov et al. 1997a, Legrand et al. 1997). Studies of stellar populations in Seyfert

galaxies and AGN (cf. Heckman et al. 1997) may also provide new insights into stellar evolution in metal rich environments.

9.3. Future applications

With the results from such analyses of stellar populations in hand, additional studies of the starburst phenomenon can proceed quickly. For example, based on the modelling of the WR and O populations in large numbers of starburst regions, possible variations from region to region in the the slope of the initial mass function for massive stars can be investigated (cf. Schaerer 1996c; Mas-Hesse & Kunth 1997). Also the detection-frequency of WC stars in WR galaxies could provide limits on the burst duration (cf. §3). Furthermore, the ejecta from a large population of WR stars may have a significant impact on the chemical evolution of the host galaxy (cf. Pagel et al. 1992; Esteban & Peimbert 1995; Kobulnicky et al. 1997). With detailed knowledge of the WR and O star populations in starburst regions, the possible links between the massive star content and spatial variations in metallicities can be investigated.

We envision that the present models will be used primarily to interpret the spectra of WR galaxies. These objects provide a window on the processes occurring during the youngest phases of a starburst (e.g. VC92; Contini, Davoust & Considère 1995; Conti 1996, Leitherer et al. 1996; Schaerer 1996c; González-Delgado et al. 1997, Mas-Hesse & Kunth 1997; Schaerer et al. 1997). As such, a study of their properties has relevance to our understanding of objects ranging from nearby H II regions to high redshift galaxies.

Future studies of starburst regions will move beyond the determination of the stellar populations and will focus on broader aspects of the starburst phenomenon, such as the chronology of starburst events, the initial mass function and its possible dependence on environmental effects, mixing processes in the ISM and the chemical

evolution of young systems. Obtaining a complete and consistent picture of a starburst region, incorporating both the stellar content with its radiative, mechanical and chemical output and the evolution of the ISM of the host galaxy would be a major goal of these efforts. Our models should provide a first step toward this goal.

We thank Paul Crowther, Laurent Drissen and Alex de Koter for kindly providing us with measurements from their spectra. We also thank Paul for answering a number of questions regarding WR line fluxes. DS wishes to thank Rosa González-Delgado, Yuri Izotov, Daniel Kunth, Enrique Pérez, and Trinh Thuan for fruitful discussions. Thierry Contini, Claus Leitherer and Georges Meynet also provided comments on a earlier version of the manuscript. DS is supported by the Swiss National Foundation of Scientific Research and acknowledges partial support from the Directors Discretionary Research Fund of the STScI. WDV acknowledges support in the form of a fellowship from the Beatrice Watson Parrent Foundation.

A. Appendix

The results from the models presented in this work are available in electronic format. Additional data such as spectral energy distributions and integrated colors are also provided. Further variations of the major input parameters (IMF slope etc.) are also considered. The models are found on the Web at <http://www.stsci.edu/ftp/science/starburst>.

REFERENCES

- Allen, S.W. 1995, MNRAS, 276, 947
- Aller, L.H. 1984, *Physics of Thermal Gaseous Nebulae*, Dordrecht: Reidel, 102
- Arnault, Ph., Kunth, D., & Schild, H. 1989, A&A, 224, 73
- Braun, H., & Langer, N. 1995, A&A, 297, 483
- Brownsberger K.R. 1995, PhD thesis, University of Colorado, USA
- Cerviño, M., & Mas-Hesse, J.M. 1994, A&A, 284, 749
- Cerviño, M., & Mas-Hesse, J.M. 1996, in *From Stars to Galaxies: The Impact of Stellar Physics on Galaxy Evolution*, ASP Conf. Series 98, Eds. C. Leitherer, U. Fritze - von Alvensleben, J. Huchra, p. 218
- Cerviño, M., Mas-Hesse, J.M., & Kunth, D. 1996, in *Wolf-Rayet Stars in the Framework of Stellar Evolution*, 33rd Liège Int. Astroph. Coll., eds. J.M. Vreux et al., (Liège: Université de Liège), p. 613
- Conti, P.S. 1991, ApJ, 377, 115
- Conti, P.S. 1996, in *The Interplay Between Massive Star Formation, the ISM, and Galaxy Evolution*, eds. D. Kunth, B. Guiderdoni, M. Heydari-Malayeri, T.X. Thuan (Gif-sur Yvette: Editions Frontières), p. 37
- Conti, P.S., & Massey, P. 1989, ApJ, 337, 251
- Conti, P.S., & Vacca W. D. 1990, AJ, 100, 431
- Contini, T., Davoust, E., & Considère, S. 1995, A&A, 303, 440
- Copetti, M.V.F., Pastoriza, M.G., & Dottori, H.A. 1986, A&A, 156, 111
- Crowther, P.A. 1997, private communication
- Crowther, P. A., Bohannan, B., & Pasquali, A. 1997, *Boulder Munich Workshop II: Properties of Hot Luminous Stars*, ed. I. Howarth, ASP Conf. Series, in press
- Crowther, P. A., & Dessart, L. 1997, MNRAS, submitted
- Dalton, W.W., & Sarazin, C.L. 1995, ApJ, 448, 369
- de Koter, A. 1996, private communication
- de Koter, A., Heap, S.R., & Hubeny, I. 1997, ApJ, 477, 792

- Dessart, L., & Crowther, P. A. 1997, Boulder Munich Workshop II: Properties of Hot Luminous Stars, ed. I. Howarth, ASP Conf. Series, in press
- Díaz, A.I. 1988, MNRAS, 231, 57
- Drissen, L. 1997, private communication
- Drissen, L., Moffat, A.F.J., & Shara, M.M. 1993, AJ, 105, 1400
- Drissen, L., Moffat, A.F.J., Walborn, N.R., & Shara, M.M. 1995, AJ, 110, 2235
- Doherty, R. M., Puxley, P. J., Lumsden, S. L., & Doyon, R. 1995, MNRAS, 277, 577
- de Loore, C., & Vanbeveren, D. 1994, A&A, 292, 463
- Eenens, P.R.J., & Williams, P.M. 1992, MNRAS, 255, 227
- Esteban, C., & Peimbert, M. 1995, A&A, 300, 78
- Ferland, G.J. 1980, PASP, 92, 596
- García-Vargas, M. 1996, From Stars to Galaxies: The Impact of Stellar Physics on Galaxy Evolution, ASP Conf. Series 98, eds. C. Leitherer, U. Fritze - von Alvensleben, & J. Huchra, p. 244
- García-Vargas, M., Bressan, A., & Díaz, A.I. 1995, A&AS, 112, 13
- Garmany, C. D. & Stencel, R. E. 1992, A&AS, 94, 211
- Garnett, D.R., Kennicutt R.C., Chu, Y.-H., & Skillman, E.D. 1991, ApJ, 373, 458
- González-Delgado, R.M., Leitherer, C., Heckman, T., & Cerviño, M. 1997, ApJ, 483, 705
- Gräfener G., Hamann, W.-R., Hillier, D.J., & Koesterke, L. 1997, A&A, in press
- Hamann, W.R., Koesterke, L., & Wessolowski, U. 1993, A&A, 274, 397
- Heckman, T. M., Gonzalez-Delgado, R., Leitherer, C., Meurer, G. R., Krolik, J., Wilson, A. S., Koratkar, A., & Kinney, A. 1997, ApJ, 482, 114
- Huchra, J.P., 1977, ApJ, 217, 928
- Hunter, D.A., & Thronson Jr., H.A. 1995, ApJ, 452, 238
- Izotov, Y.I., & Thuan, T.X., 1997, ApJ, submitted
- Izotov, Y.I., Dyak, A.B., Chaffee, F.H., Foltz, C.B., Kniazev, A.Y., & Lipovetsky, V.A. 1996, ApJ, 458, 524
- Izotov, Y.I., Thuan, T.X., & Lipovetsky, V.A. 1994, ApJ, 435, 647
- Izotov, Y.I., Thuan, T.X., & Lipovetsky, V.A. 1997a, ApJS, 108, 1
- Izotov, Y.I., Foltz, C.B., Green, R.F., Guseva, N.G., & Thuan, T.X. 1997b, ApJ, 487, L37
- Kingsburgh, R.L., & Barlow, M.J. 1995, A&A, 295, 171
- Kingsburgh, R.L., Barlow, M.J., & Storey, P.J. 1995, A&A, 295, 75
- Kobulnicky, H.A., Skillman, E.D., Roy, J.-R., Walsh, J.R., & Rosa, M.R. 1997, ApJ, 477, 679
- Koesterke L., & Hamann, W.-R. 1995, A&A, 299, 503
- Krüger, H., Fritze-v. Alvensleben, U., Fricke, K.J., & Loose, H.-H. 1992, A&A, 259, L73
- Kudritzki, R.P., 1996, in Wolf-Rayet Stars in the Framework of Stellar Evolution, 33rd Liège Int. Astroph. Coll., eds. J.M. Vreux et al., (Liège: Université de Liège), p. 467
- Kunth, D., & Joubert, M. 1985, A&A, 142, 411
- Kunth, D., & Sargent, W.L.W. 1983, ApJ, 273, 81
- Kunth, D., & Schild, H. 1986, A&A, 169, 71
- Langer, N. 1995, in Wolf-Rayet Stars: Binaries, Colliding Winds, Evolution, IAU Symp. 163, eds. K.A. van der Hucht, & P.M. Williams, (Dordrecht: Kluwer), p. 15
- Leitherer, C. 1990, ApJS, 73, 1

- Leitherer, C., & Heckman T.M. 1995, ApJS, 96, 9
- Leitherer, C., Vacca, W.D.W., Conti, P.S., Filippenko, A.V., Robert, C., & Sargent, W.L.W. 1996, ApJ, 465, 717
- Legrand, F., Kunth, D., Roy, J.-R., Mas-Hesse, J.M., & Walsh, J.R. 1997, A&A, in press
- Lundström, I. & Stenholm, B. 1984, A&AS, 58, 163
- Maeder, A. 1982, A&A, 105, 149
- Maeder, A. 1991a, A&A, 242, 93
- Maeder, A. 1991b, A&AS, 84, 139
- Maeder, A., & Conti, P.S. 1994, ARA&A, 32, 227
- Maeder, A., Lequeux, J., & Azzopardi, M. 1980, A&A, 90, 117
- Maeder, A., & Meynet, G. 1994, A&A, 287, 803
- Mas-Hesse, J.M., & Kunth, D. 1991a, A&AS, 88, 399
- Mas-Hesse, J.M., & Kunth, D. 1991b, in Wolf-Rayet Stars and Interrelations with Other Stars in Galaxies, IAU Symp. 143, eds. K. A. van der Hucht, & B. Hidayat, (Dordrecht: Kluwer), p. 613
- Mas-Hesse, J.M., & Kunth, D. 1997, A&A, submitted
- Massey, P., Johnson, K.E., & DeGioia-Eastwood, K. 1995a, ApJ, 454, 151
- Massey, P., Lang, C.C. Degioia-Eatwood, K., & Garmany, C.D. 1995b, ApJ, 438, 188
- Meynet, G. 1995, A&A, 298, 767
- Meynet, G., Maeder, A., Schaller, G., Schaerer, D., & Charbonnel, C. 1994, A&AS, 103, 97
- Moffat, A. F. J. 1983, A&A, 124, 273
- Morris, P.W. 1995, PhD thesis, University of Colorado, USA
- Morris, P.W., Brownsberger, K. R., Conti, P. S., Massey, P., & Vacca, W. D. 1993, ApJ, 412, 324
- Olive, K.A., Skillman, E., & Steigman G. 1997, ApJ, 483, 788
- Olofsson, K. 1995, A&AS, 111, 57
- Osterbrock, D.E. 1989, *Astrophysics of Gaseous Nebulae and Active Galactic Nuclei*, Univ. Science Books, California
- Pagel, B.E.J., Simonson, E.A., Terlevich, R.J., & Edmunds, M.G. 1992, MNRAS, 255, 325
- Philips, A.C., & Conti, P.S. 1992, ApJ, 395, 91
- Roy, J.-R., Aubé, M., McCall, M.L., & Dufour, R.J. 1992, ApJ, 386, 498
- Salpeter, E.E. 1955, ApJ, 121, 161
- Schaerer, D. 1996a, A&A, 309, 129
- Schaerer, D. 1996b, in From Stars to Galaxies: The Impact of Stellar Physics on Galaxy Evolution, ASP Conf. Series 98, eds. C. Leitherer, U. Fritze - von Alvensleben, J. Huchra, p. 174
- Schaerer, D. 1996c, ApJ, 467, L1
- Schaerer, D., & de Koter, A. 1997, A&A, 322, 598
- Schaerer, D., de Koter, A., Schmutz, W., & Maeder, A. 1996a, A&A, 310, 837
- Schaerer, D., de Koter, A., Schmutz, W., & Maeder, A. 1996b, A&A, 312, 475
- Schaerer, D., Contini, T., Kunth D., & Meynet, G. 1997, ApJ, 481, L75
- Schaerer, D., & Vacca, W.D., 1996, in WR Stars in the Framework of Stellar Evolution, 33rd Liège Int. Astroph. Coll., eds. J.M. de Vreux et al. (Liège: Université de Liège), p. 641
- Schaller, G., Schaerer, D., Meynet, G., & Maeder, A. 1992, A&AS, 96, 269
- Schmutz, W., 1991, in Stellar Atmospheres: Beyond Classical Limits, eds. L. Crivellari, I. Hubeny, D.G. Hummer, NATO ASI Series C, Vol. 341, p. 191
- Schmutz, W., Leitherer, C., & Gruenwald, R. 1992, PASP, 104, 1164
- Seaton, M. J. 1979, MNRAS, 187, 73P

- Shields, J.C. 1993, *ApJ*, 419, 181
- Smith, L.F. 1991, in *Wolf-Rayet Stars and Interrelations with Other Stars in Galaxies*, IAU Symp. 143, eds. K. A. van der Hucht & B. Hidayat, (Dordrecht: Kluwer), p. 601
- Smith, L.F., & Maeder, A. 1991, *A&A*, 241, 77
- Smith, L.F., & Maeder, A. 1997, *A&A*, in preparation
- Smith L.F., Meynet G., & Mermilliod J.-C. 1994, *A&A*287, 835
- Smith, L.F., Shara, M.M., & Moffat, A.F.J. 1990a, *ApJ*, 348, 471 (SSM90a)
- Smith, L.F., Shara, M.M., & Moffat, A.F.J. 1990b, *ApJ*, 358, 229 (SSM90b)
- Smith, L.F., Shara, M.M., & Moffat, A.F.J. 1996, *MNRAS* 281, 163 (SSM96)
- Stasińska, G., & Leitherer, C. 1996, *ApJS*, 107, 661
- Stasińska, G., & Schaerer, D. 1997, *A&A*, 322, 615
- Terlevich, E., Díaz, A. I., Terlevich, R., González-Delgado, R. M., Pérez, E., & García Vargas, M. L. 1996, *MNRAS*, 279, 1219
- Vacca, W.D. 1992, PhD thesis, University of Colorado
- Vacca, W.D. 1994, *ApJ*, 421, 140
- Vacca, W.D., & Conti, P.S. 1992, *ApJ*, 401, 543 (VC92)
- Vacca, W. D., & Conti, P. S. 1997, in prep.
- Vacca, W.D., Garmany, C.D., & Shull, M.J. 1996, *ApJ*, 460, 914
- Vacca, W. D., Robert, C., Leitherer, C., & Conti, P. S. 1995, *ApJ*, 444, 647
- Vanbeveren, D. 1995, *A&A*, 294, 107
- Vanbeveren, D., Van Bever, J., & De Donder, E. 1997, *A&A*, 317, 487

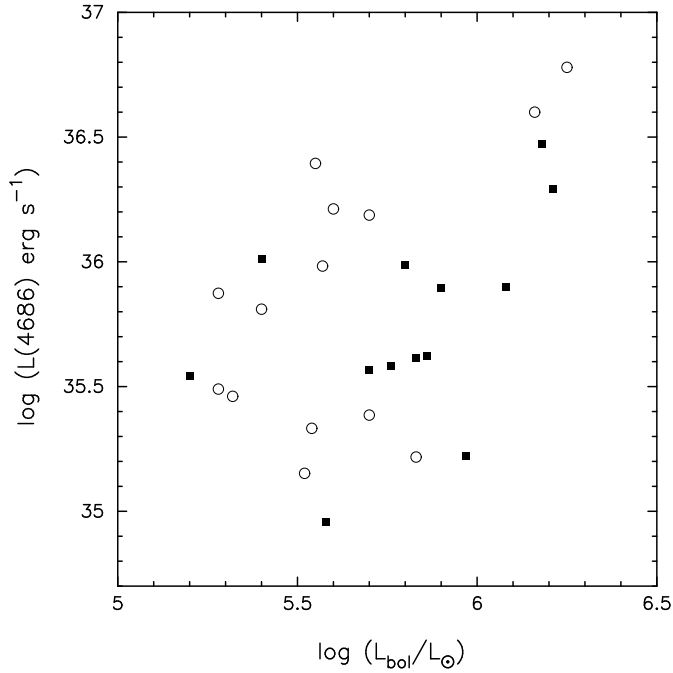


Fig. A1.— Luminosity in the He II 4686 line vs. the bolometric luminosity for WNL stars, from the measurements and analysis by Crowther & Dessart (1997). Open circles denote LMC stars; filled squares are Galactic stars. Note the huge variation in line luminosity across the WNL subclass.

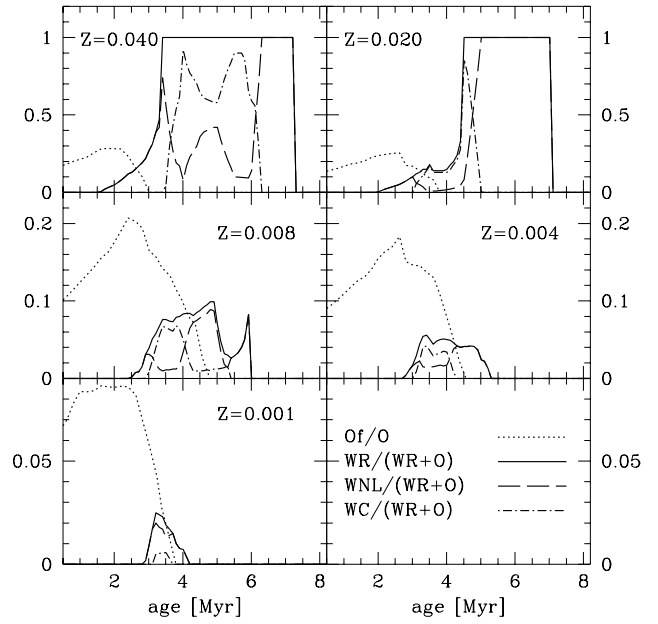


Fig. A2.— Predicted Of/O and WR/O star number ratios as a function of age for all metallicities. All models are calculated for an instantaneous burst with a Salpeter IMF. Shown are the total WR/(WR+O) (solid), the WNL/(WR+O) (dashed), the WC/(WR+O) (dashed-dotted), and the Of/O number ratios. Note the change of the ordinate between the top, middle, and lower panels.

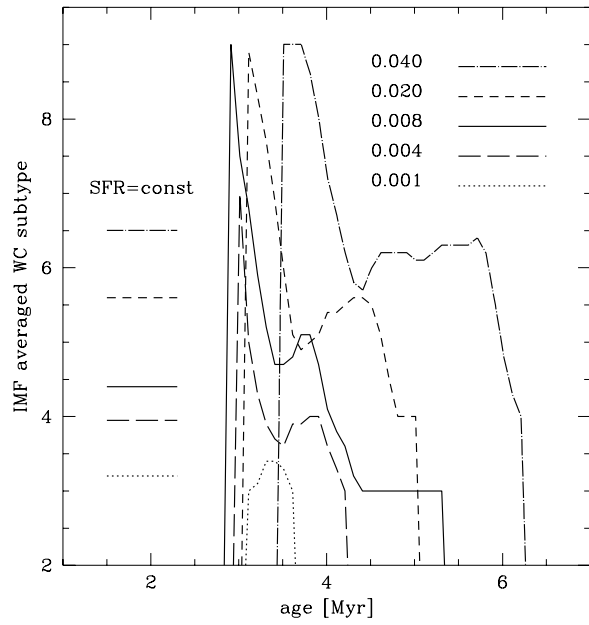


Fig. A3.— Temporal evolution of the IMF-averaged WC subtype for all metallicities ($Z=0.040$: dashed-dotted, 0.020 : short dashed, 0.008 : solid, 0.004 : long dashed, 0.001 : dotted). WO stars are designated by a WC3 subtype

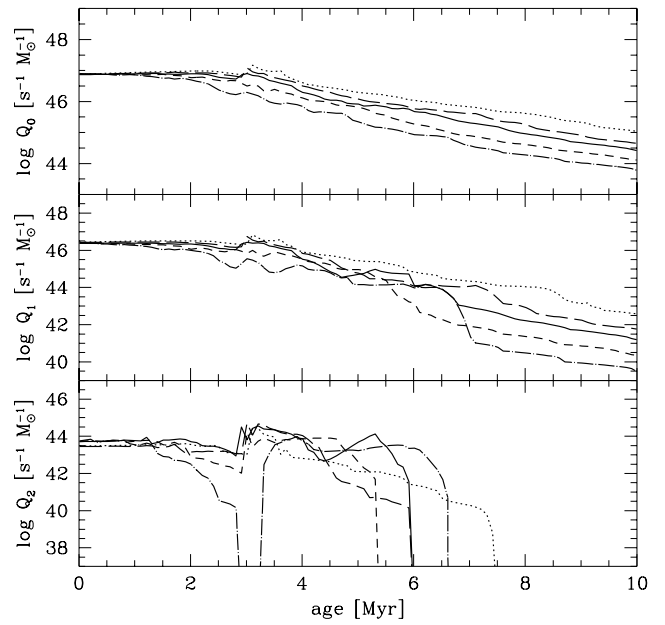


Fig. A4.— Temporal evolution of the ionizing photon flux of a stellar population (normalised to a total mass of $1 M_{\odot}$) for all metallicities. *Top panel*: Lyman continuum flux, *Middle*: Flux in the He I continuum, *Lower panel*: flux in the He II continuum. Same symbols as in Fig. A3

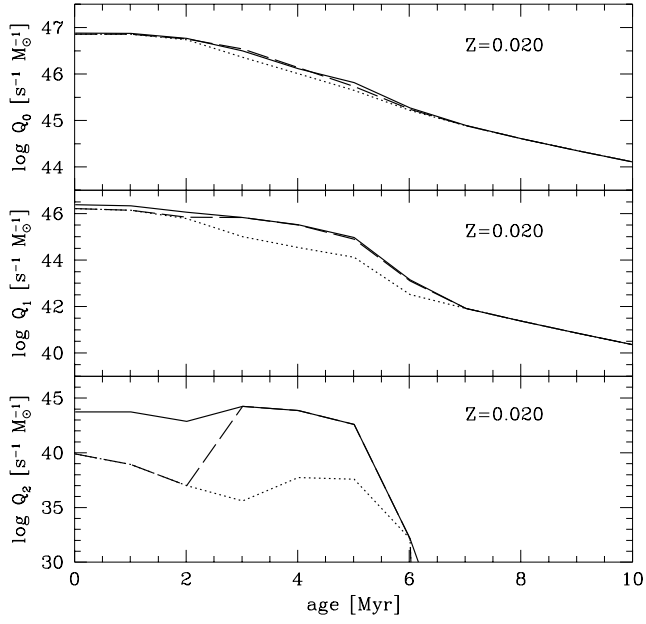


Fig. A5.— Comparison of predicted ionizing fluxes using different atmosphere models. Shown is the standard model for $Z=0.020$. Dotted: using plane parallel, LTE, line blanketed models of Kurucz (1992) only; Dashed: same as dotted but using spherically expanding non-LTE models for WR stars (Schmutz, Leitherer & Gruenwald, 1992); Solid: same as dashed but using spherically expanding, line blanketed, non-LTE *CoStar* models for O stars. The top, middle, and bottom panel show Q_0 , Q_1 , and Q_2 respectively

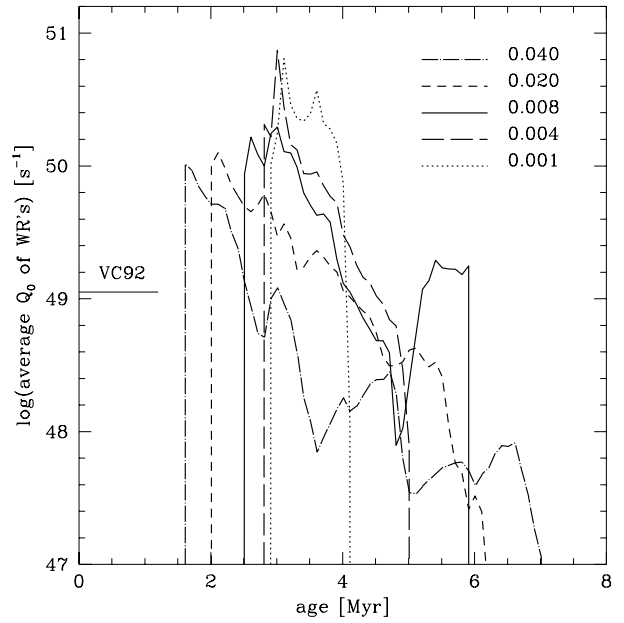


Fig. A6.— Time evolution of the average Lyman continuum luminosity provided per WR star in instantaneous burst models. The thin solid horizontal line indicates the value of Q_O^{WNL} from Vacca & Conti (1992). Same symbols as in Fig. A3

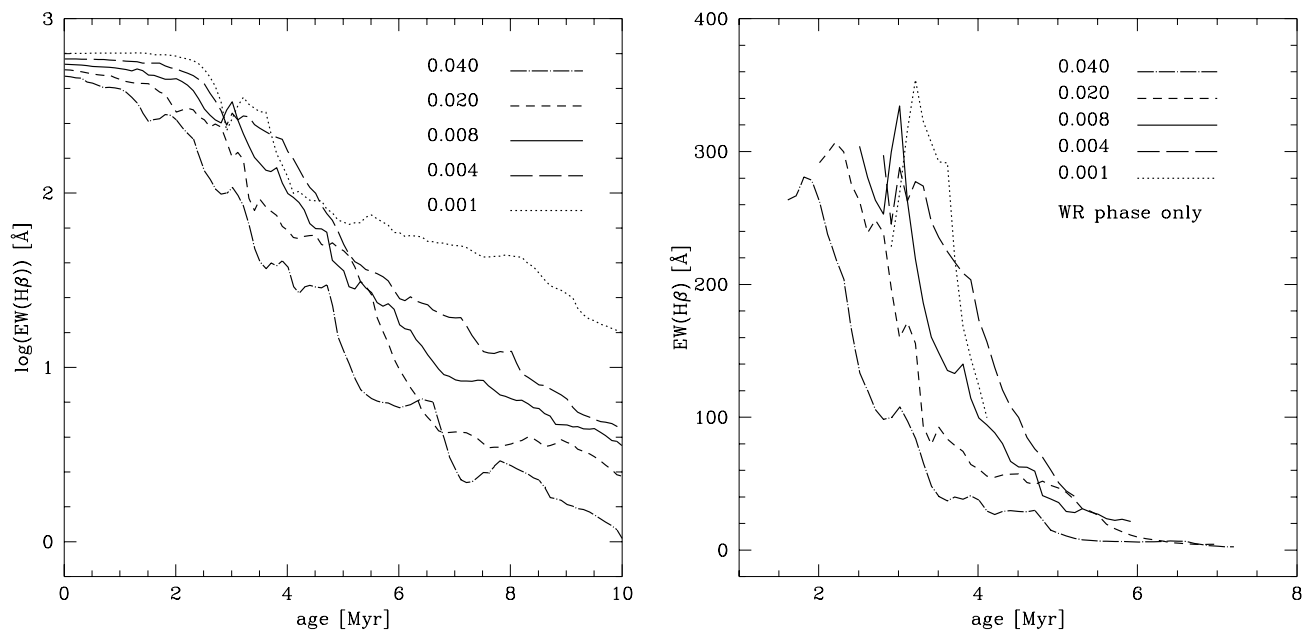


Fig. A7.— Time evolution of the H β equivalent width for an instantaneous burst at the given metallicity. Same symbols as in Fig. A3. *Left panel:* Logarithm of $W(\text{H}\beta)$ for ages from 0 to 10 Myr. *Right panel:* Evolution of $W(\text{H}\beta)$ during the WR rich phases of the burst. Horizontal lines on the margins show the maximum/minimum $W(\text{H}\beta)$ during the WR phase

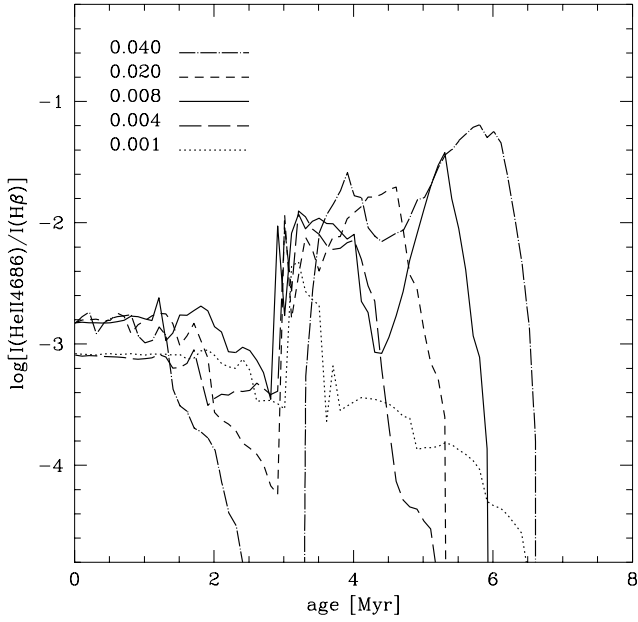


Fig. A8.— Predicted *nebular* emission line ratio of He II $\lambda 4686/H\beta$ as a function of age. Same symbols as in Fig. A3. See Figs. A13 and A16 for the total WR and nebular 4686 emission

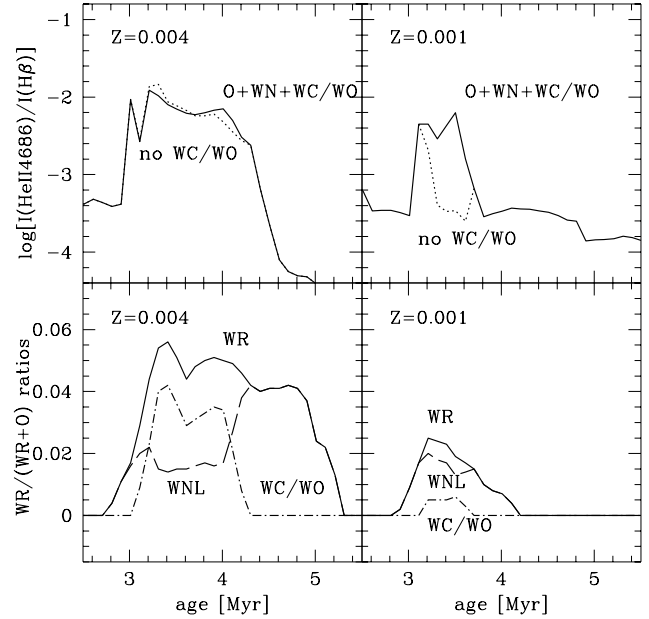


Fig. A9.— *Lower panels:* total WR/(WR+O) (solid lines), WNL/(WR+O) (dashed), and WC/(WR+O) (dashed-dotted) number ratios as a function of time for $Z=0.004$ (left) and $Z=0.001$ (right). *Upper panels:* Nebular He II $\lambda 4686/H\beta$ as a function of age for $Z=0.004$ (left) and $Z=0.001$ (right). The dotted lines show the predicted He II $\lambda 4686/H\beta$ when WC stars are excluded. This shows that both WC and (hot) WN stars contribute to the nebular He II emission

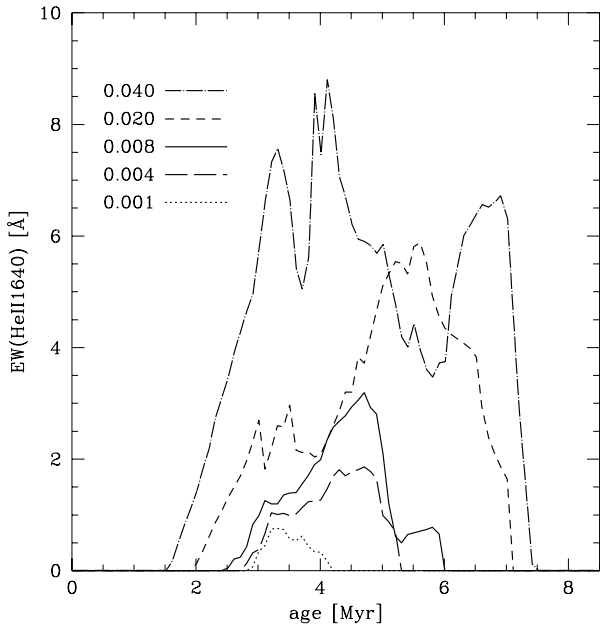


Fig. A10.— Evolution of the He II $\lambda 1640$ equivalent width. Same symbols as in Fig. A3

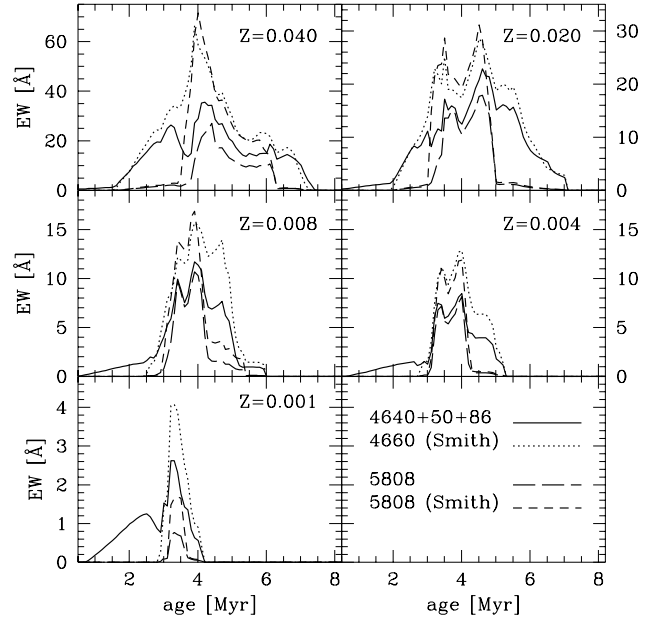


Fig. A11.— Evolution of WR bump equivalent widths for all metallicities. Solid lines: 4660 bump including N III/v $\lambda 4640$, C III/IV $\lambda 4650$, and He II $\lambda 4686$. Long-dashed: C IV $\lambda 5808$. Both following the prescriptions in Tables 1 and 2. Dotted and short-dashed lines show the WR bump equivalent widths using the prescriptions of Smith (1991; cf. Table 3)

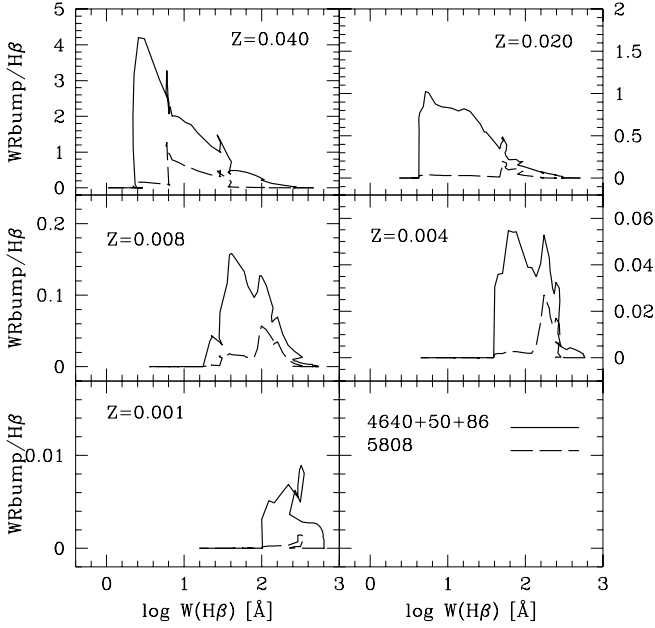


Fig. A12.— Evolution of WR bump intensities relative to $H\beta$ for all metallicities. Solid: 4660 bump, long-dashed: C IV $\lambda 5808$, computed as in Fig. A11. The less accurate values using the prescription of Smith (1991) is not shown here. Certain cases show non-uniqueness of line intensities when plotted against $W(H\beta)$ (e.g. for $Z=0.001$, but cf. also other Figs.). This behaviour is due to the slight increase of the $H\beta$ with time at the beginning of the WR phase (see Fig. A7), which is in turn related to the contribution of WR stars to the Lyman continuum flux

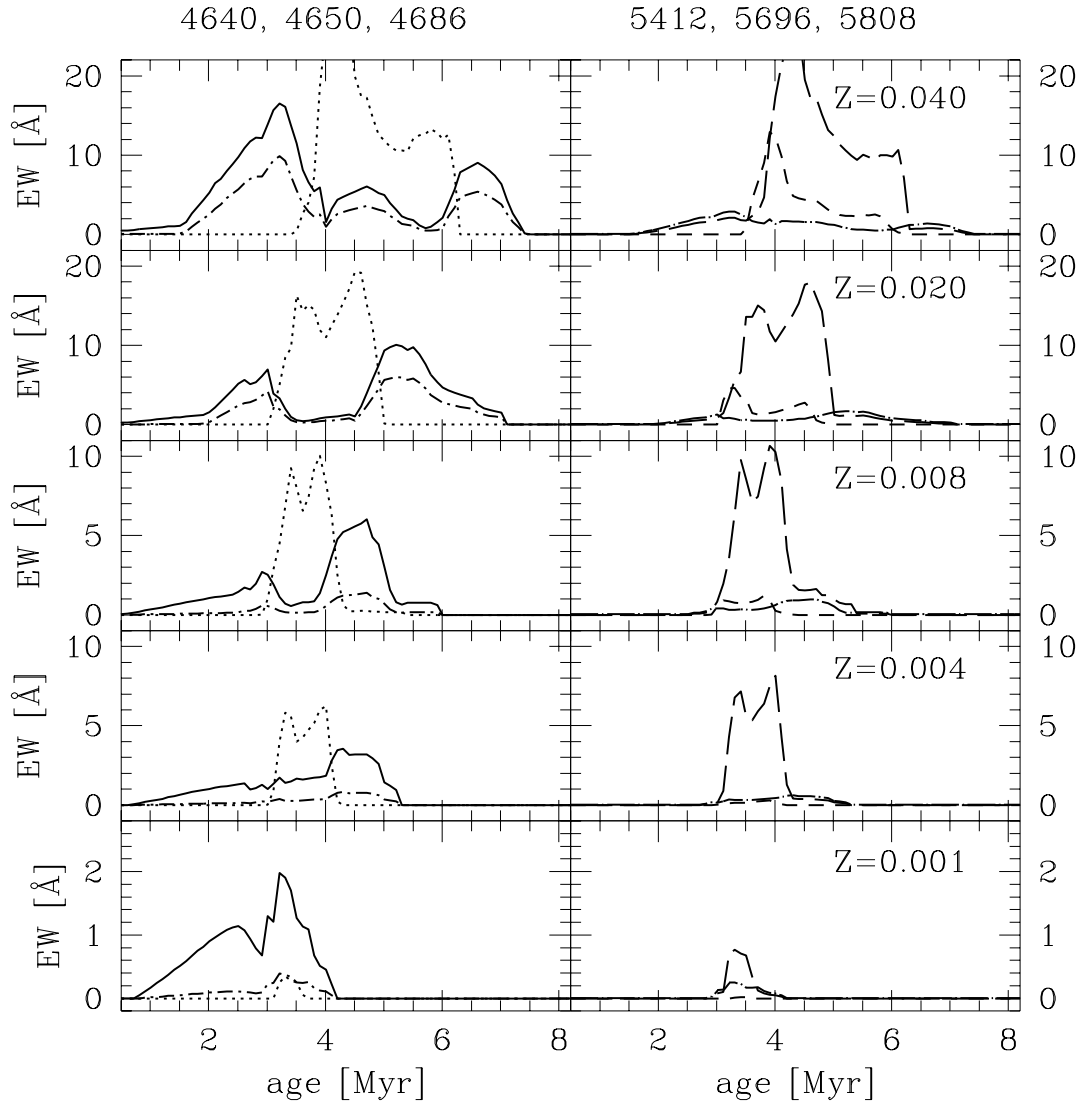


Fig. A13.— Predicted equivalent widths of optical WR lines for all metallicities. *Left panels:* He II λ 4686 (solid), C III/IV λ 4650 (dotted), N III/V λ 4640 (short dashed-dotted). *Right panels:* C IV λ 5808 (long dashed), C III λ 5696 (short dashed), He II λ 5412 (long dashed-dotted)

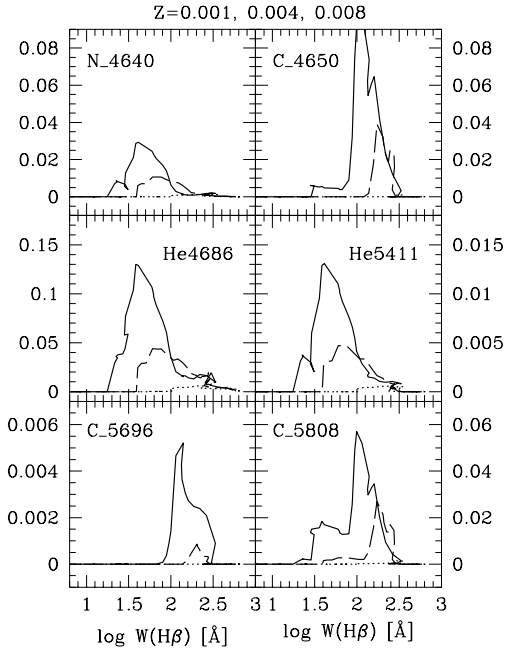


Fig. A14.— Predicted intensity ratio $I(\lambda)/I(H\beta)$ for WR lines at $Z=0.008$ (solid), 0.004 (long-dashed), and 0.001 (dotted)

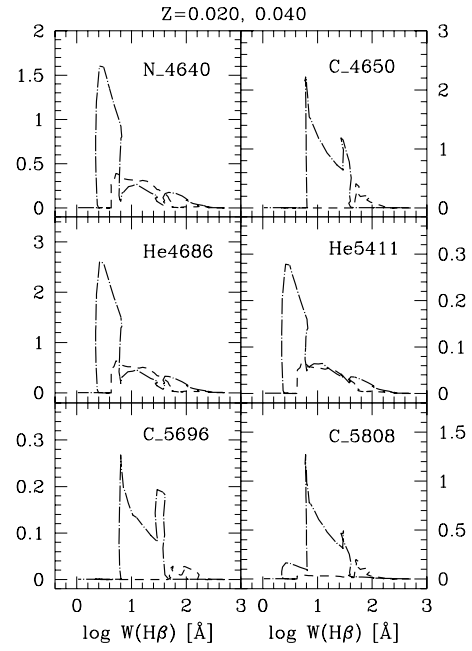


Fig. A15.— Same as Fig. A14 for $Z=0.02$ (short-dashed) and 0.04 (dashed-dotted)

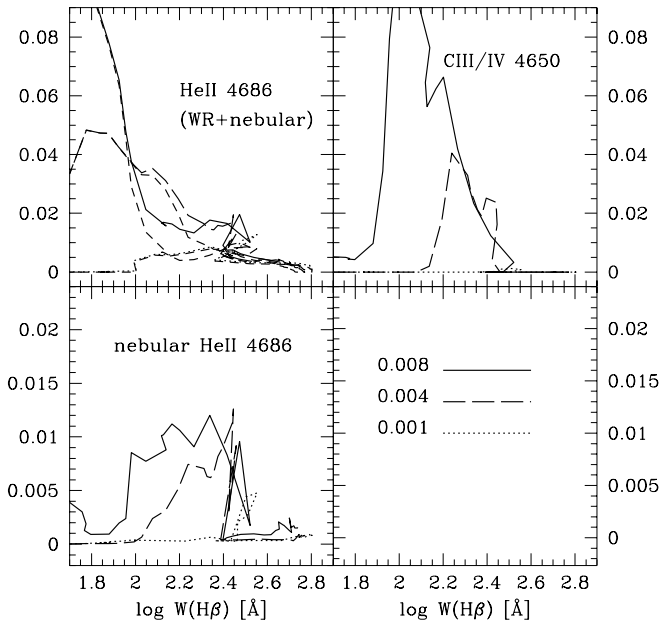


Fig. A16.— Predicted intensity ratios $I(\lambda)/I(H_\beta)$ for nebular and WR lines at $\lambda \sim 4650\text{-}4700 \text{ \AA}$ for $Z=0.008$ (solid), 0.004 (long-dashed), and 0.001 (dotted)

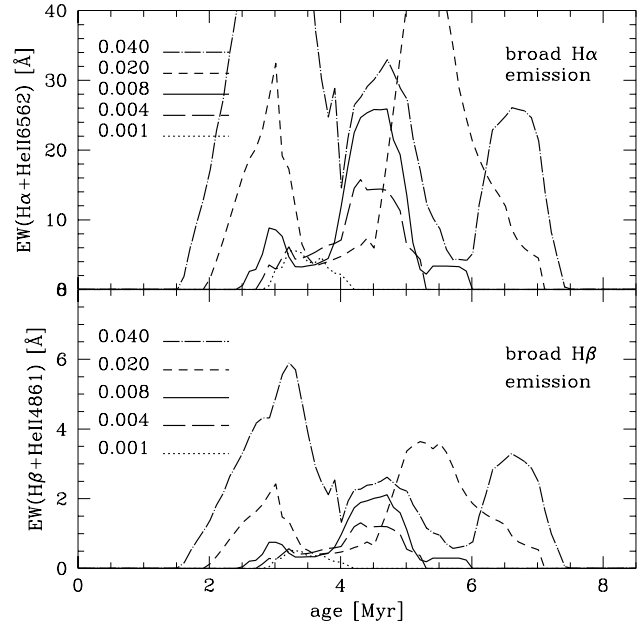


Fig. A17.— Predicted equivalent widths of $H\alpha$ (upper panel) and $H\beta$ (lower panel) blends for all metallicities. Symbols as in Fig. A3

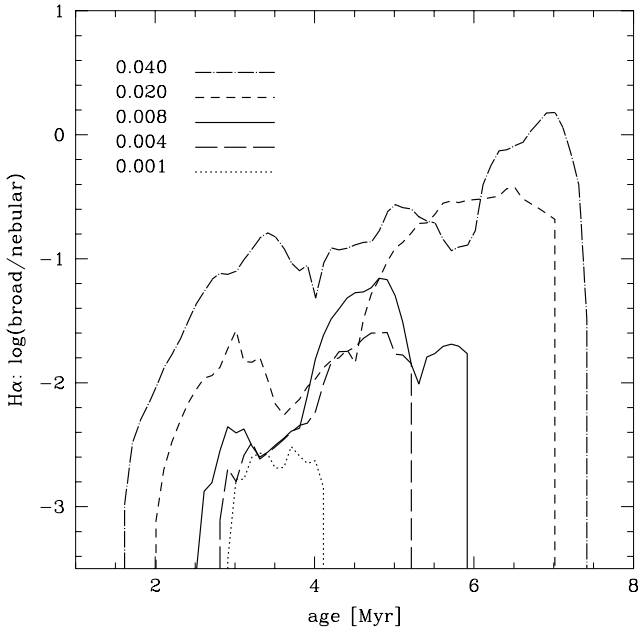


Fig. A18.— Ratio of broad WR emission to nebular $H\alpha$ line for all metallicities. Symbols as in Fig. A3. The relative contribution to $H\beta$ is nearly identical to the $H\alpha$ contribution (see § 6.2.4)

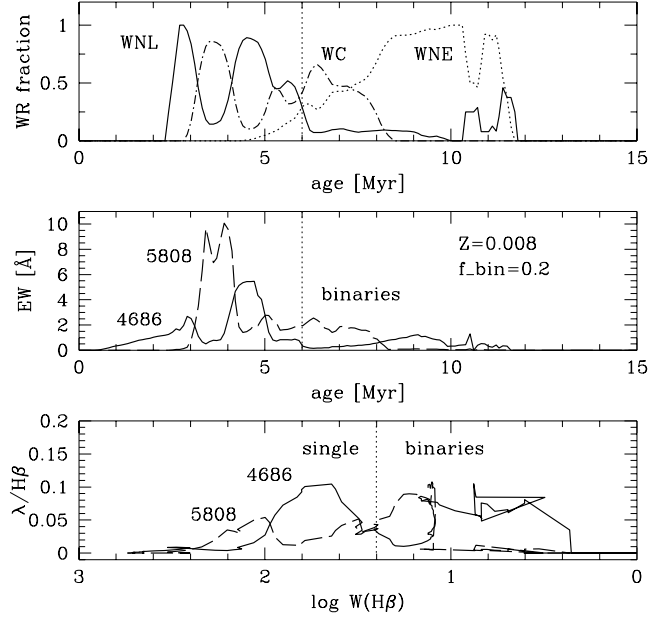


Fig. A19.— Model predictions including massive close binary stars with a binary fraction $f = 0.2$ for $Z=0.008$ (instantaneous burst). *Top panel:* Relative fraction of WR stars of different subtypes. *Middle:* Temporal evolution of predicted equivalent widths for He II $\lambda 4686$ (solid) and C IV $\lambda 5808$ (long-dashed). The arrow indicates the beginning of the phase where WR stars are predominantly formed through the binary channel. *Lower panel:* Line ratios $\lambda/H\beta$ as a function $W(H\beta)$. Same symbols as middle panel. The vertical dotted lines illustrates the clear separation of the “single star” and “binary” phases in this diagram

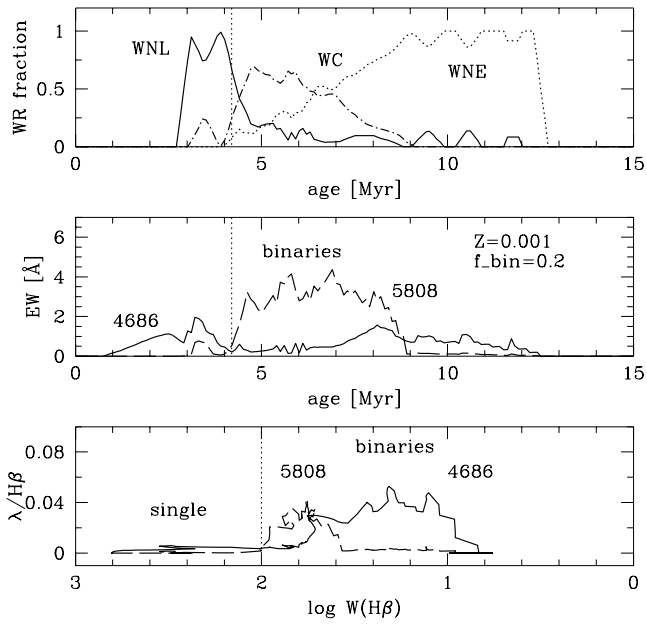


Fig. A20.— Same as A19 for $Z=0.001$

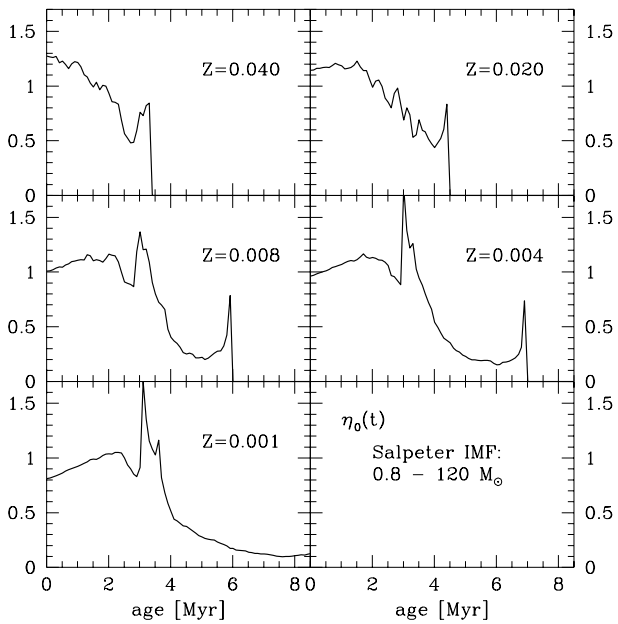


Fig. A21.— Evolution of $\eta_0(t)$ (defined by Eq. 12) in standard burst models for metallicities from $Z=0.040$ to 0.001

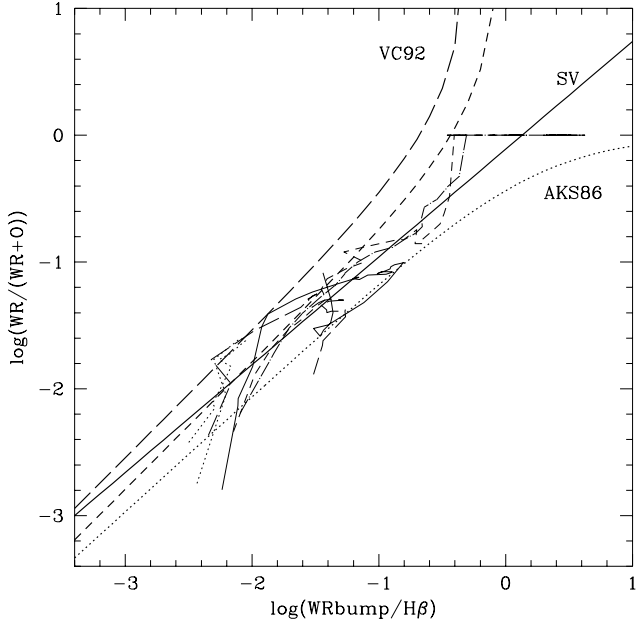


Fig. A22.— Number ratio $WR/(WR+O)$ as a function of the intensity ratio of the WR-bump over $H\beta$ obtained from instantaneous burst models at all metallicities (thin lines using same symbols as in Fig. A3). The thick solid line (SV) shows the fit to our models (cf. Eq. 17). Thick dashed: relation from Arnault, Kunth & Schild. Thick long-dashed: relation from VC92 (their Eq. 15 assuming $\eta = 1.$). Thick short-dashed: same as long-dashed but assuming a larger average line luminosity of $\log(4650-4686)=36.7$

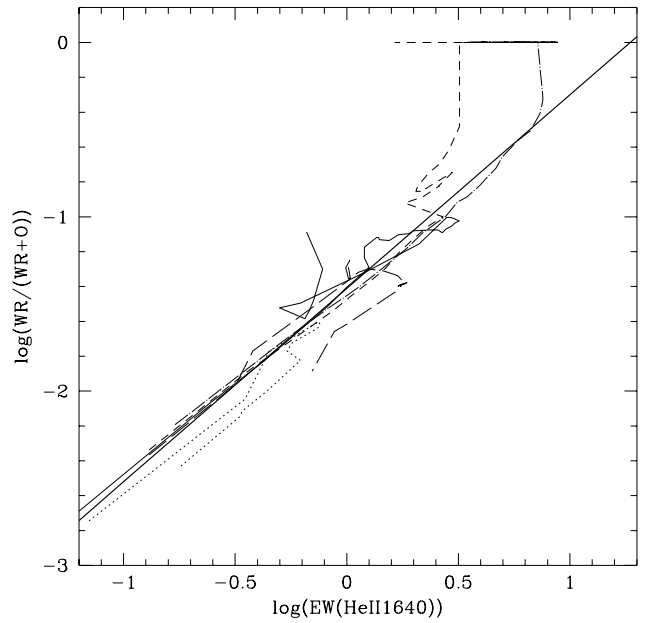


Fig. A23.— Number ratio $WR/(WR+O)$ as a function of the He II $\lambda 1640$ equivalent width (emission, in \AA) obtained from instantaneous burst models at all metallicities (thin lines using same symbols as in Fig. A3). The thick solid line shows the fit to our models (cf. Eq. 18)